

NATURAL RUBBER FILMS REINFORCED WITH
CELLULOSE AND CHITOSAN PREPARED BY LATEX
AQUEOUS MICRODISPERSION



Miss Naipaporn Sutipanwihan

จุฬาลงกรณ์มหาวิทยาลัย
CHULALONGKORN UNIVERSITY

A Thesis Submitted in Partial Fulfillment of the Requirements
for the Degree of Master of Engineering in Chemical Engineering
Department of Chemical Engineering
FACULTY OF ENGINEERING
Chulalongkorn University
Academic Year 2021
Copyright of Chulalongkorn University

แผนยงธรรมเนียมที่ถูกรเสริมแรงด้วยเซลลูโลสและไคโตซาน เตรียมโดยการกระจายตัวระดับไม
โครในน้ำยง



วิทยานิพนธ์นี้เป็นส่วนหนึ่งของการศึกษาตามหลักสูตรปริญญาวิศวกรรมศาสตรมหาบัณฑิต
สาขาวิชาวิศวกรรมเคมี ภาควิชาวิศวกรรมเคมี
คณะวิศวกรรมศาสตร์ จุฬาลงกรณ์มหาวิทยาลัย
ปีการศึกษา 2564
ลิขสิทธิ์ของจุฬาลงกรณ์มหาวิทยาลัย

นัยน์ปพร สุนิพันธ์วิหาร : แผ่นยางธรรมชาติที่ถูกเสริมแรงด้วยเซลลูโลสและไคโตซาน เตรียมโดยการกระจายตัวระดับไมโครในน้ำยาง. (NATURAL RUBBER FILMS REINFORCED WITH CELLULOSE AND CHITOSAN PREPARED BY LATEX AQUEOUS MICRODISPERSION) อ.ที่ปรึกษาหลัก : ศ. ดร.เหมือนเดือน พิศาลพงศ์

พลาสติกเป็นหนึ่งในผลิตภัณฑ์ที่ได้จากปิโตรเลียม ซึ่งมีการใช้กันอย่างแพร่หลายทั่วโลก เนื่องจากมีคุณสมบัติที่หลากหลาย อย่างไรก็ตาม ขยะพลาสติกจำนวนมากสร้างมลภาวะต่อสิ่งแวดล้อม เนื่องจากองค์ประกอบที่เป็นพิษ และไม่สามารถย่อยสลายได้ทางชีวภาพ ดังนั้นจึงมีการเสนอการใช้วัสดุธรรมชาติทดแทนการใช้วัสดุจากปิโตรเลียมสำหรับการผลิตพลาสติกชีวภาพ ยางธรรมชาติเป็นวัสดุที่ได้จากธรรมชาติ ที่มีคุณสมบัติโดดเด่นในเรื่องของความยืดหยุ่นสูง ยางธรรมชาติยังมีข้อเสียบางประการ เช่น มีความต้านทานแรงดึงต่ำและความต้านทานการเสียดสีต่ำ นอกจากนี้ การใช้งานยังมีข้อจำกัดเนื่องจากทนต่อน้ำมันและตัวทำละลายได้ไม่ดี ดังนั้นการปรับปรุงคุณสมบัติทางกายภาพ เช่น ความแข็ง โมดูลัส หรือความต้านทานการเสียดสี จึงเป็นสิ่งจำเป็นที่ต้องปรับปรุงคุณสมบัติของยางธรรมชาติ

ในงานวิจัยนี้ พลาสติกยางธรรมชาติ ถูกเสริมแรงด้วยเซลลูโลส และไคโตซาน เพื่อปรับปรุงคุณสมบัติเชิงกล เคมี และชีวภาพ พลาสติกไคโตซานที่มีน้ำหนักโมเลกุล 30,000 กรัม/โมล และ 500,000 กรัม/โมล ถูกนำมาใช้ในศึกษา พลาสติกคอมโพสิต CE/CH/NR สามารถเตรียมได้ด้วยวิธีการกระจายตัวระดับไมโครในน้ำยาง ที่มีอัตราส่วนความเข้มข้นที่แตกต่างกันของน้ำยางธรรมชาติต่อเซลลูโลสต่อไคโตซาน (NR: CE: CHS/CHL) พลาสติกคอมโพสิต CE/CH/NR ถูกนำไปตรวจสอบคุณสมบัติทางกายภาพ เคมี และชีวภาพ ผลของการวิเคราะห์ด้วยเทคนิค ฟลูออโรกราฟฟีทรีมอินฟราเรดสเปกโตรสโคปี แสดงให้เห็นถึงปฏิสัมพันธ์ของพันธะไฮโดรเจนระหว่างเซลลูโลสและไคโตซานในฟิล์มคอมโพสิต และพบว่าคุณสมบัติเชิงกล ความต้านทานแรงดึงและ โมดูลัสของฟิล์มคอมโพสิตเหล่านี้มีค่าสูงขึ้นจากการเสริมแรงด้วยเซลลูโลสและไคโตซาน พบว่ามีค่าความต้านทานแรงดึงสูงสุดเท่ากับ 13.8 MPa และค่าโมดูลัสสูงสุดเท่ากับ 12.74 MPa จากคอมโพสิตฟิล์มที่เสริมแรงด้วยเซลลูโลสความเข้มข้น 10% โดยน้ำหนัก และไคโตซานที่ความเข้มข้น 10% โดยน้ำหนัก ค่าการยืดหยุ่นสูงสุดเท่ากับ 526% ในคอมโพสิตฟิล์มที่เสริมแรงด้วยเซลลูโลสเข้มข้น 10% โดยน้ำหนักและไคโตซาน 5% โดยน้ำหนัก การเติมเซลลูโลสและไคโตซานยังช่วยเพิ่มประสิทธิภาพในการยับยั้งจุลชีพ (100% สำหรับ *E. coli* และ 99% สำหรับ *S. aureus*) และเพิ่มความสามารถในการทนต่อสารเคมีและตัวทำละลายที่ไม่มีขั้วของฟิล์มคอมโพสิต ซึ่งจากคุณสมบัติต่าง ๆ นั้นฟิล์มคอมโพสิตยางธรรมชาติมีศักยภาพที่ดี ในการนำไปใช้เป็นผลิตภัณฑ์ที่มีความยืดหยุ่นสูง และบรรจุภัณฑ์ที่มีความเป็นมิตรต่อธรรมชาติ

สาขาวิชา วิศวกรรมเคมี
ปีการศึกษา 2564

ลายมือชื่อนิสิต

ลายมือชื่อ อ.ที่ปรึกษาหลัก

6272048421 : MAJOR CHEMICAL ENGINEERING

KEYWORD: Natural rubber; Cellulose; Chitosan; Composite film

Naipaporn Sutipanwihan : NATURAL RUBBER FILMS REINFORCED WITH CELLULOSE AND CHITOSAN PREPARED BY LATEX AQUEOUS MICRODISPERSION. Advisor: Prof. Dr. MUENDUEN PHISALAPHONG

Plastics are one of the derived products from petroleum material, which have been used in many applications worldwide, because of their various properties. However, plastic wastes create toxic environmental pollutions and problems because of their toxic constituents and non-biodegradability. Accordingly, nature materials have been proposed as a substitute for petroleum materials for bioplastic production. Natural rubber (NR) is a product from natural, which is well-known for its high elasticity. However, there are some drawbacks such as low tensile strength and low abrasion resistance. Moreover, its applications are also limited because of its poor resistance to oil and solvents. Therefore, the improvement of physical properties such as hardness, Young's modulus, or abrasion resistance is required to improve the properties of NR.

In this study, In order to improve mechanical, chemical, and biological properties, natural rubber (NR) films were reinforced with cellulose (CE) and chitosan (CH). Chitosan powders at a molecular weight of 30,000 g/mol (CHS) and 500,000 g/mol (CHL) were used for the study. The CE/CH/NR composite films were successfully prepared via a latex aqueous microdispersion method with a different weight ratio of NR: CE: CHS/CHL. The CE/CH/NR composite films were characterized for physical, chemical, and biological properties. Fourier transform infrared spectroscopy (FTIR) results demonstrated strong interactions of hydrogen bonds between CE and CHS/CHL in the composite films. The tensile strength and the modulus of the composite films in dried forms were found to increase with the reinforcement of CE and CHS/CHL. The maximum tensile strength (13.8 MPa), Young's modulus (12.74 MPa) were obtained from the composite films reinforced with CE at 10 wt% and CHS at 10 wt%. The maximum elongation at 526% was obtained from the composite films reinforced with CE at 10 wt% and CHL at 5.0 wt%. The addition of CE and CHS/CHL could also promote antimicrobial activities (100% for *E. coli* and 99% for *S. aureus*) and chemical resistance against non-polar solvents of the composite films. The NR composites films have potential uses as high elasticity NR products and green-polymer packaging.

จุฬาลงกรณ์มหาวิทยาลัย
CHULALONGKORN UNIVERSITY

Field of Study: Chemical Engineering
Academic Year: 2021

Student's Signature
Advisor's Signature

ACKNOWLEDGEMENTS

This thesis is not completed if without support from many parts.

Firstly, I would like to express my deepest gratitude to Professor Dr. Muenduen Phisalaphong, my advisor, for her valuable advice and kind encouragement throughout this research work.

Secondly, I am sincerely thankful to Dr. Phuet Prasertcharoensuk, The thesis committee chairman, Dr. Chutimon Satirapipathkul, and Dr. Jeerun Kingkraew, the thesis committee member, for their useful critiques of this research work and helpful suggestions.

A special thanks to comments, kindness, and friendship from all student members of Professor Dr. Muenduen Phisalaphong groups as well as my friends in the lab of Chemical Engineering Research Unit for Value Adding of bioresources. I would like to express my appreciation to staff from Department of Chemical Engineering, Chulalongkorn University for their kindness and help.

Special thanks will go to all my friends and colleagues for friendship and encouragement as well as stimulating intellectual environment to work and study in the Faculty of Chemical Engineering, Chulalongkorn University.

Finally, I must also thank my parents and friends for their immense support and help during this project. Without their help, completing this project would have been very difficult.

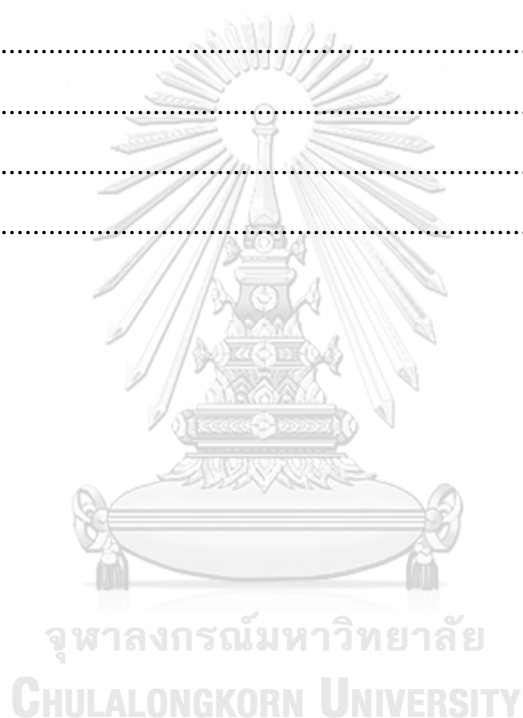
Naipaporn Sutipanwihan

TABLE OF CONTENTS

	Page
.....	iii
ABSTRACT (THAI)	iii
.....	iv
ABSTRACT (ENGLISH).....	iv
ACKNOWLEDGEMENTS.....	v
TABLE OF CONTENTS.....	vi
LIST OF TABLES.....	ix
LIST OF FIGURES	x
CHAPTER I.....	1
1.1 Introduction.....	1
1.2 Research objectives	2
1.3 Research scopes	2
CHAPTER II.....	4
2.1 THEORY	4
2.1.1 Natural rubber latex.....	4
2.1.2 Chitosan.....	4
2.1.3 Cellulose.....	5
2.1.4 Polymer blending	5
2.1.5 Bioplastic film	6
2.2 LITERATURE REVIEW	7
2.2.1 Mechanically Reinforced Chitosan/Cellulose Nanocrystals Composites with Good Transparency and Biocompatibility	7
2.2.2 Mechanical properties of chitosan and natural rubber latex.....	8
2.2.3 Chitosan and Natural Rubber Latex Biocomposite Prepared by Incorporating Negatively Charged Chitosan Dispersion.....	9

2.2.4 Reinforcement of Natural Rubber with Bacterial Cellulose via a Latex Aqueous Microdispersion Process	10
2.2.5 Sustainable development of natural rubber and its environmentally friendly composites	11
2.2.6 Electron beam irradiation cross linked chitosan/ natural rubber-latex film: Preparation and characterization.	13
2.2.7 A Clean and Sustainable Cellulose-Based Composite Film Reinforced with Waste Plastic Polyethylene Terephthalate	14
2.2.8 A review on mechanical and water absorption properties of polyvinyl alcohol based composites/films.....	15
2.2.9 Preparation and properties of natural rubber/chitosan microsphere blends	16
CHAPTER III	18
3.1 Material.....	18
3.2 Methods	18
3.3 Characterization of physical, biological and chemical properties of the natural rubber films reinforced with cellulose and chitosan.....	19
3.3.1 Scanning Electron Microscope and Energy Dispersive X-ray Spectrometer (SEM-EDS).....	19
3.3.2 Fourier Transform Infrared Spectroscopy (FTIR).....	19
3.3.3 Mechanical Properties Testing	20
3.3.4 Thermal Gravimetric Analysis (TGA)	20
3.3.5 Differential Scanning Calorimetry (DSC).....	20
3.3.6 X-Ray Diffraction (XRD)	20
3.3.7 Contact angle	20
3.3.8 Water Absorption Capacity (WAC)	20
3.3.9 Toluene Uptake (TU)	21
3.3.10 Antibacterial	21
CHAPTER IV	22
4.1 Scanning electron microscopy (SEM).....	22
4.2 Fourier-transform infrared spectroscopy (FTIR).....	24

4.3 Mechanical properties.....	25
4.4 Thermal Gravimetric Analysis (TGA).....	29
4.5 Differential scanning calorimetry (DSC).....	32
4.6 X-Ray Diffraction (XRD).....	34
4.7 Contact angle	37
4.8 Water Absorption Capacity (WAC)	38
4.9 Toluene Uptake (TU).....	39
4.10 Antibacterial ability	41
CHAPTER V	44
CONCLUSION.....	44
REFERENCES	45
VITA.....	51



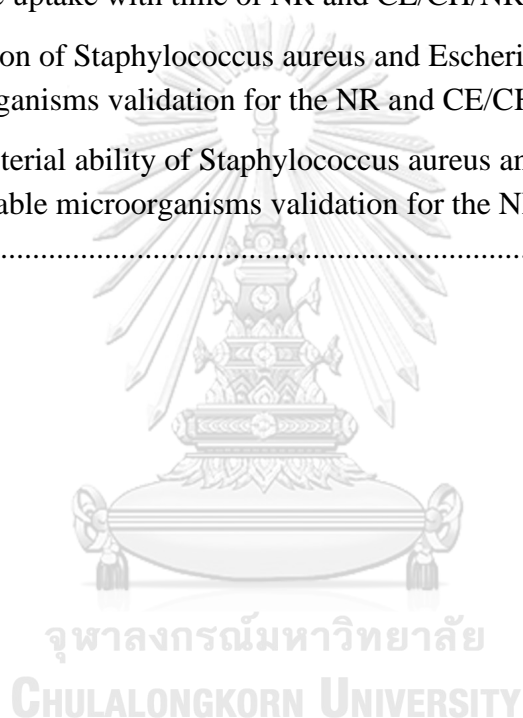
LIST OF TABLES

	Page
Table 1. The Type of Properties for Polymer Blends (22).....	6
Table 2. The comparison of reinforcing improvement in NR products with various renewable organic reinforcing fillers (25).	12
Table 3. Mechanical properties of PVA based composites (36).....	15
Table 4. Effect of CS loadings on mechanical properties of CS/NR blends (40).....	16
Table 5. Antibacterial properties of chitosan/natural rubber films with different chitosan microsphere loadings (40).	17
Table 6. The composition of microfibrillated cellulose-chitosan-natural rubber (CE/CH/NR) composite films.....	19
Table 7. The crystallite sizes of NR and NR composite films.....	35
Table 8 Calculation of degree of crystallinity.....	36
Table 9 .Degree of dynamic water contact angles (°) of NR, CE, CHL, CHS and CE/CH/NR composites.	37
Table 10 The clear zone of Staphylococcus aureus and Escherichia coli for determining the viable microorganisms validation for the NR and CE/CH/NR composite films.....	43

LIST OF FIGURES

	Page
Figure 1. Natural rubber latex structure (3)	4
Figure 2. Chitosan structure (18)	5
Figure 3. Structure of cellulose (19)	5
Figure 4 Sketch of the possible microstructure of the obtained CS/CNCs composites.(16).....	8
Figure 5 Typical stress-strain curve for CS/CNCs with different CNCs weight contents at room temperature and the Young's modulus as function of CNCs content at room temperature (CS/CNCs-0.5 wt% means CS/CNCs composite with 0.5 wt% CNCs.)(16).....	8
Figure 6. The stress–strain curves of Cs/NR (26).....	9
Figure 7. Model of preparation of chitosan dispersion in the natural rubber latex/chitosan compound (13).....	10
Figure 8. Elastic modulus (E') of the NR/CT biocomposites with CT loading from 0 to 8 phr(13).	10
Figure 9 Degree of crystallinity and mechanical properties of NR, BC, and NRBC composites.(7).....	11
Figure 10. Stress-strain curve of NR, BC, and NRBC composites (7).....	11
Figure 11. Mechanism of vulcanization of NR (a) sulfur vulcanization (b) EB vulcanization (34).	13
Figure 12. Tensile strength of CS/NR latex-film (a) effect of vulcanization (b) effect of CS loading and radiation dose (34).	14
Figure 13. MC/PET mass ratio (RMC:PET) dependent on tensile strength of the neat MC film and MC/PET films (35).....	14
Figure 14 MC/PET mass ratio (RMC:PET) dependent on breaking.(35).....	15
Figure 15. SEM images of the films of NR, CE/CH/NR composites: (a) surface views , (b) cross section views	23
Figure 16. FTIR spectra of NR, CHS, CHL, CE and NR composite films	25
Figure 17. a) Tensile strength b) Elongation at break c) Modulus of composite films as a function of the weight ratio of cellulose and chitosan in NR composites.	28

Figure 18 Thermal gravimetric analysis (TGA) curves of NR, CE, CH and CE/CH/NR composite films.	31
Figure 19 Derivative Thermogravimetry (DTG) curves of NR, CE, CH and CE/CH/NR composite films.	31
Figure 20 DSC chromatograms of NR, CE, CH and CE/CH/NR composites.....	33
Figure 21 X-ray diffraction (XRD) patterns of CE, CH, and CE/CH/NR films.....	35
Figure 22 Water absorption capacity (WAC %) with time of NR and CE/CH/NR composite films.....	39
Figure 23 Toluene uptake with time of NR and CE/CH/NR composite films	40
Figure 24 Reduction of Staphylococcus aureus and Escherichia coli for determining the viable microorganisms validation for the NR and CE/CH/NR composite films. ..	42
Figure 25 Antibacterial ability of Staphylococcus aureus and Escherichia coli for determining the viable microorganisms validation for the NR and CE/CH/NR composite films.....	42



CHAPTER I INTRODUCTION

1.1 Introduction

Plastics are one of the derived products from petroleum hydrocarbons, which have been used in many applications worldwide, because of their various properties such as, outstanding formability in various shapes, low cost, and corrosion resistance(1). However, plastic wastes create toxic environmental pollutions and problems because of their toxic constituents and non-biodegradability. Accordingly, natural materials have been proposed as a substitute for petroleum based materials for bioplastic production, because of their notable advantages such as renewable resource and biodegradability. In addition, bioplastics have been reported for better elasticity and elongation properties than petrochemical plastics.(2)

Southern Thailand is the world's largest producer and exporter of natural rubber (NR) products from rubber plants (*Hevea brasiliensis*). NR is well-known for its high elasticity, which is the ability to regain its original shape after being deformed; however, it is easily decomposed by high temperature, ultraviolet or ozone. Therefore, the improvement of physical properties such as hardness, Young's modulus or abrasion resistance is required to enhance the properties of NR(3).

Properties of NR composites can be improved by addition of reinforcing materials. For considerable environmental benefits, the reinforcing materials in NR matrix should be environmentally friendly, biodegradable, and nontoxic such as, starch, clay, fiber, wood flour, oil palm flour, cotton fiber, and microcrystalline cellulose (4). Cellulose is the most abundant resources of biopolymer on earth. It is an organic polymer with straight chain polymer, which can be obtained from plants, algae, and bacteria. Cellulose microfibrils have several hydroxyl groups on the linear chain. It can form hydrogen bonds with oxygen atoms on the same or a neighbor chain to the high strength (5; 6). Many research works of NR reinforcement by using cellulose as bio material filler have been reported (6). The result showed that the increased tensile strength and Young's modulus were obtained in agreement with the increase in the amount of cellulose, but the considerable decrease in the elongation at break was observed (7).

Chitosan is a natural product extracted from chitin by deacetylation pathway. It is the second most abundant natural polysaccharide after cellulose. It has a very similar chemical structure to that of cellulose, except that one of the hydroxyl (-OH) groups is substituted by an amine(-NH₂) group. The various functional groups of cellulose and chitosan can form hydrogen bonds between each other.(8) Chitosan has many advantages such as, biodegradability, nontoxicity, renewable resource and antimicrobial activity, which can be used in many applications (9; 10). From the research of cellulose-chitosan antibacterial composite films, the addition of chitosan could increase elongation at break in biocomposite film (11). Moreover, cellulose-

chitosan blended materials contained many useful properties such as, antibacterial activity, good mechanical characteristics, high adsorption capacities, high porosity, metal ions adsorption, barrier properties, etc (12). The presence of chitosan in the biocomposite of chitosan and NR latex resulted in an increased elastic modulus (E') in conjunction with enhanced antibacterial activity against *Staphylococcus aureus* (13). In order to improve overall mechanical properties and antimicrobial characteristics, NR composites reinforced with cellulose and chitosan are developed in this study by using a latex aqueous microdispersion method. The properties of the developed composites are characterized for further consideration of their potential use.

1.2 Research objectives

- To fabricate natural rubber films reinforced with cellulose and chitosan via latex aqueous microdispersion.

- To characterize physical, biological and chemical properties of the natural rubber films reinforced with cellulose and chitosan.

1.3 Research scopes

1.3.1 Study the effects of micro cellulose fibers and chitosan as reinforcing agents for NR composite films.

- Effects of concentration ratio of natural rubber latex, chitosan and cellulose on properties of NR composite films are investigated.

- The sheets paper of cellulose from eucalyptus pulp were kindly provided by the Teppattana Paper Mill Co., Ltd. (Bangkok, Thailand). The sheets were dried in an oven at 80 °C for 24 h to remove moisture prior to using in the experiment. The microfibrillated cellulose (CE) was prepared by crushing the dried cellulose sheet, grinding by using ball mill (PM 100, Haan, Germany), and sieving, respectively. After grinding, the size of CE particle is in the range of 10–30 μm , with the average particle size of 26.5 μm (evaluated by using Laser particle size distribution (PSD)).

- Chitosan products at low molecular weight (MW 30,000, DAC 90%) and high molecular weight (MW 500,000, DAC 90%) were used for the study.

1.3.2 Characterize the physical, biological and chemical properties of the natural rubber films reinforced with cellulose and chitosan

- Fourier Transform Infrared Spectroscopy (FTIR)
- Scanning Electron Microscope and Energy Dispersive X-ray Spectrometer (SEM-EDS)
- Mechanical Properties Testing
- Thermal Gravimetric Analysis (TGA)
- Differential Scanning Calorimetry (DSC)
- X-Ray Diffraction (XRD)

- Contact angle
- Water Absorption Capacity (WAC)
- Toluene Uptake (TU)
- Antibacterial



CHAPTER II THEORY & LITERATURE REVIEW

2.1 THEORY

2.1.1 Natural rubber latex

Natural rubber latex (NR) is harvested mainly from *Hevea brasiliensis* or others. It is a sticky, milky colloid drawn off by making incisions in the bark. NR is a colloidal mixture comprising of rubber particles dispersed in water. NR particle consists of isoprene units (C_5H_8) with a double bond in the cis-1,4-polyisoprene configuration (Figure 1). A molecular weight of NR is 100,000- 1,000,000 daltons (14; 15). The advantages of products from NRL are high elasticity and flexibility (3). It is used extensively in many applications (gloves, condoms, and baby bottle teats). It has a large stretch ratio and high resilience. However, it has disadvantage such as poor solvent resistance, low modulus, barrier properties, electrical properties and easily deformation. Therefore, reinforcement fillers are required to improve the disadvantages of the material. Reinforcing agents are such as, silica, cellulose, graphene oxide, chitosan (16). Researches on sustainable fillers in NR composites used cellulose derived from tunicates to produce cellulose nanocrystals in order to increase the mechanical properties and the thermal stability of NR (17).

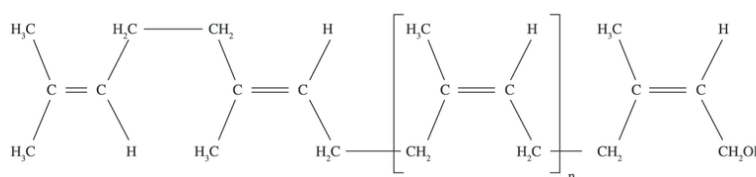


Figure 1. Natural rubber latex structure (3)

2.1.2 Chitosan

Chitosan (poly-1, 4-D-glucosamine) is a natural polymer extracted from chitin. Chitin can be found in shrimp shells, squid cores, and crab shells etc. Chitosan is produced from chitin by the removal of acetyl groups (Deacetylation) with concentrated alkalis. In the chemical structure, chitin has acetamido ($-NHCOCH_3$) as a function group. The deacetylation reaction changes acetamido ($-NHCOCH_3$) into amino group ($-NH_2$) (Figure 2) (18). The degree of deacetylation and molecular weight (MW) of chitosan affect the properties and applications of chitosan. The MW affects the whiteness of the polymer strings and it leads to the solubility of chitosan in acetic acids. If chitosan has high MW, it has a long polymer string. On the other hand, if chitosan has low MW, it has a short polymer string. Chitosan normally dissolves well in organic acids such as acetic acid, propanoic acid, lactic acid etc. In the present, chitosan has many applications because of many special properties of chitosan, which are nontoxic, biocompatible, biodegradable, good mechanical strength (9; 10) and environment friendly. Chitosan powder can be dissolved in acetic acid solution to form a viscous liquid. It can be molded into many forms such as gels, films, tablets,

fibers, coatings, membranes. Moreover, chitosan can effectively control the growth and reproduction of hazardous bacteria and also control toxic (16).

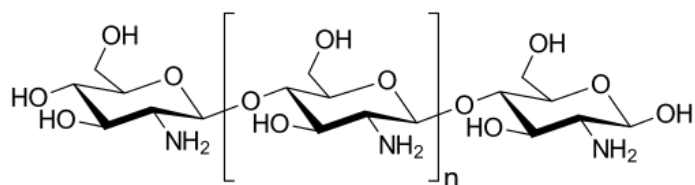


Figure 2. Chitosan structure (18)

2.1.3 Cellulose

Cellulose is a polysaccharide consisting of a linear chain of β(1→4) linked D-glucose units (Figure 3) (19). It is an organic compound with the chemical formula (C₆H₁₀O₅)_n. Cellulose is the most abundant biomaterials (environment friendly, natural resource) on the earth (6). Cellulose can be biosynthesized from plants, many forms of algae and bacteria. It is hydrophilic. Cellulose is a crystalline solid, which has a white powdery appearance. It has high tensile strength due to hydrogen bonds between the individual chains in cellulose microfibrils. The alternate arrangement of glucose molecules in cellulose contributes to the high tensile strength of cellulose (20). The tensile strength of cellulose microfibrils is comparable to steel. It is insoluble in water and organic solvents. According to the many beneficial properties of natural cellulose fibers such as good mechanical strength, wide availability, low density, low price and renewability, cellulose is frequently used as a reinforcing material (21).

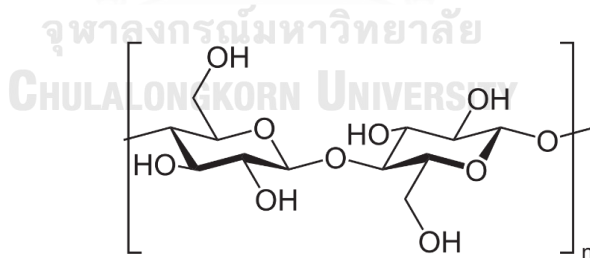


Figure 3. Structure of cellulose (19)

2.1.4 Polymer blending

Polymer blend is a very popular and easily method of modifying polymer properties by blending at least two polymers together to create a new material with different properties. The objective of polymer blending is to develop new products with the property which cannot be attained from individual constituents. The polymer blend gives the good properties of each species by mixing them together homogeneous (22).

Thermodynamics of Polymer Blends (22)

Complete miscibility in a mixture of two polymers requires that the following condition is fulfilled:

$$\Delta G_m = \Delta H_m - T\Delta S_m < 0$$

Where ΔG_m is the Gibb's free energy, ΔH_m is the enthalpy and ΔS_m and entropy of mixing at temperature T, respectively.

Types of polymer blends

1. Miscible polymer blends
2. Compatible polymer blends
3. Immiscible polymer blends

Table 1. The Type of Properties for Polymer Blends (22)

Type	Miscible Blends	Partially Miscible Blends	Immiscible Blends
Phase	Homogenous	Partial phase separation	Complete phase separation
Mechanical properties	components averaged	individual component polymers mostly retained	Poor interface leading
Gibb's free energy	$\Delta G < 0$	$\Delta G > 0$	$\Delta G > 0$
Glass transition temperatures	They show a single glass transition.	They show two glass transition temperatures, intermediate to the component polymers	They show the two glass transition temperatures of the component polymers

2.1.5 Bioplastic film

Bioplastics are plastic material produced from biological materials instead of petroleum. It is also often called bio-based plastic which is biodegradable by natural microorganisms and bacteria. It is plastic material produced from raw materials in nature sources (renewable sources) such as sugar cane, cassava, pea protein, corn, etc. with the origin of natural raw materials. Bioplastics are usually derived from sugar derivatives, including starch, cellulose, and lactic acid. Generally, bioplastic films are made from polysaccharide (starch, alginate, cellulose ethers,

chitosan, carrageenan) exhibit good gas barrier properties. Linear structures of some of these polysaccharides get their films tough, flexible and transparent. Their films are resistant to fats and oils (23). However, owing to their hydrophilic nature, they are poor water vapor barriers. Among biopolymers in general, polysaccharide is considered to be one of the most promising materials for use in biodegradable plastics (24). Moreover, a limiting barrier to the development of polysaccharide is the brittle nature of film containing high concentrations of starch. because it easily becomes rigid and brittle during long time storage, and therefore, loses its value in use.(25)

2.2 LITERATURE REVIEW

2.2.1 Mechanically Reinforced Chitosan/Cellulose Nanocrystals Composites with Good Transparency and Biocompatibility

Geng et al. (16) developed chitosan/cellulose nanocrystals composites. He prepared homogeneous dispersion chitosan/cellulose composite with strong interfacial interactions resulting from hydrogen bonding between CS chains and CNCs (Figure 4). He tested the mechanical properties of CS/CNCs composite. The result represented in Figure 5 shows the stress-strain curves of the CS/CNCs composites with different contents of CNCs. This pure CS performed poor mechanical behaviors (low tensile strength and Young's modulus). However, the addition of CNCs led to a significant improvement in the tensile strength and Young's modulus, and the addition of CNCs at 4 wt% was considered to be the best ratio for reinforcing CS composite films in the study. Both CS and CNCs are biocompatible materials and cell proliferation test showed that the obtained composites are noncytotoxic and could potentially meet the safety requirements of biomedical applications. These advantages pave the way for potential applications of CS in the field of commercial plastics and encourage the use of CS as environment-friendly material and biomedical material (16).

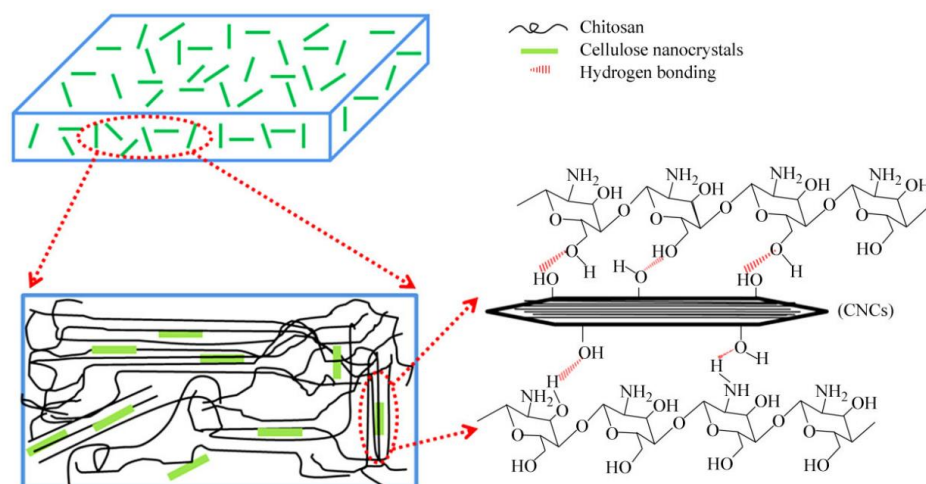


Figure 4 Sketch of the possible microstructure of the obtained CS/CNCs composites.(16)

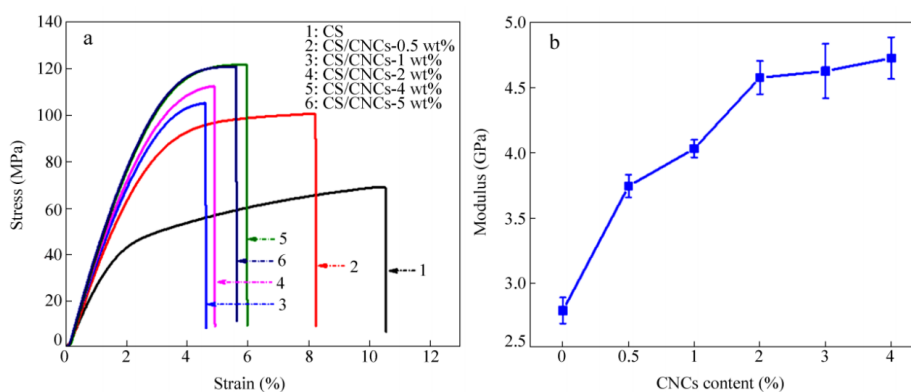


Figure 5 Typical stress-strain curve for CS/CNCs with different CNCs weight contents at room temperature and the Young's modulus as function of CNCs content at room temperature (CS/CNCs-0.5 wt% means CS/CNCs composite with 0.5 wt% CNCs.)(16)

2.2.2 Mechanical properties of chitosan and natural rubber latex

Rao et al. (26) studied the mechanical properties of thermoplastic elastomeric blends of chitosan and natural rubber latex. The composite films of chitosan and NR were prepared by varying chitosan/NR ratios and characterized for mechanical properties of film. The results showed the stress-strain curves of CS/NR are given in Figure 6. These curves illustrate the deformation pattern of different blends. The experiment had been limited to 50% Cs/NR due to the limitation of physical property as the 50% chitosan films were too brittle to perform the mechanical test. According to the graph, 35% of chitosan films gave the highest modulus and tensile strength at 1.98 MPa and 3.25 MPa, respectively. However, the elongation was decreased compared to the pure NR, which could be observed in the slope of the stress-strain curves. Moreover, the graph also showed that if the chitosan content increased, the

stress-strain curve also steadily changed from the rubbery to plastic-like property. In conclusion, the percentage of chitosan affects the limitation of chain flexibility as the graph showed that the chain flexibility of the system is more fixed when the percentage of chitosan increases (26).

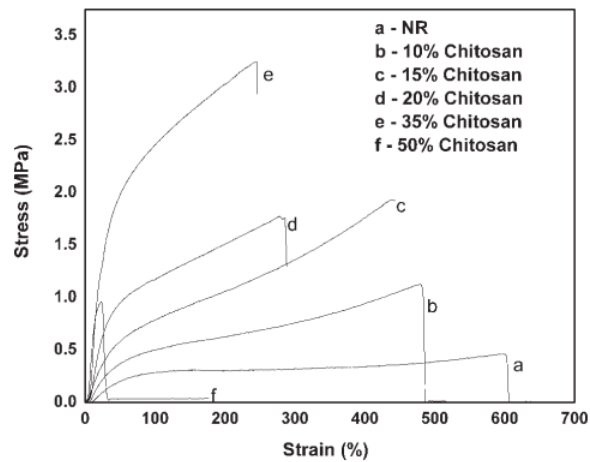


Figure 6. The stress–strain curves of Cs/NR (26)

2.2.3 Chitosan and Natural Rubber Latex Biocomposite Prepared by Incorporating Negatively Charged Chitosan Dispersion

Boonrasri et al. (13) presented a new mixing method which improved properties of the NR/CT biocomposites. Interesting point is the process of loading chitosan (from 0-8 phr) into the NR latex, which has effect on the properties of NR in the mixture. According to the experiment, chitosan powder is soluble in acetic acid. However, NR coagulated when dissolved with chitosan in acid, leading to the damage. Therefore, they must avoid dissolving chitosan in acid or need to adjust the pH before mixing with NRL. The pH of the 10% chitosan dispersion should be ≈ 10.26 in order to disperse 10% CT into NRL, in which chitosan could be incorporated into the NRL without NR coagulation. The structure of chitosan has positive charge at amino group. On the other hand, when pH is high, it causes the substance to be in a base. Chitosan's amino function as a negative charge is shown in Figure 7 (13).

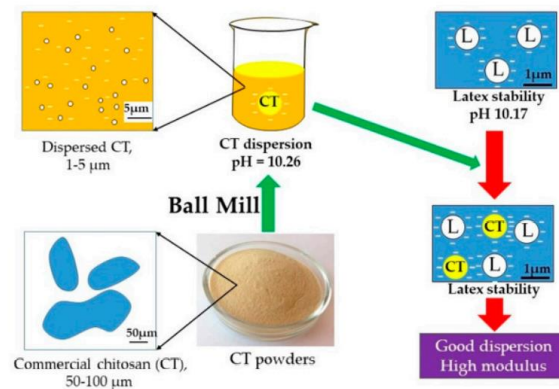


Figure 7. Model of preparation of chitosan dispersion in the natural rubber latex/chitosan compound (13).

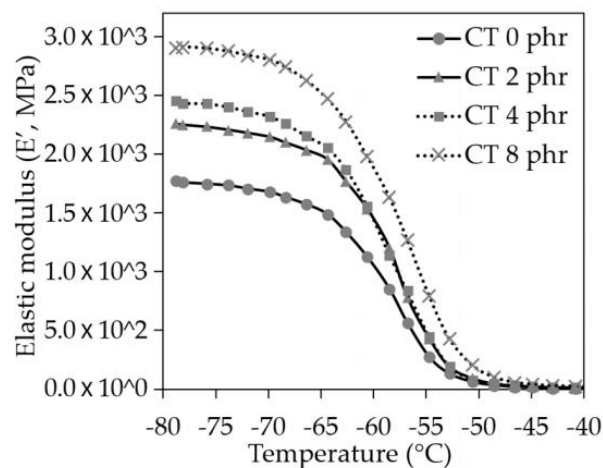


Figure 8. Elastic modulus (E') of the NR/CT biocomposites with CT loading from 0 to 8 phr(13).

Figure 8 showed the Elastic modulus (E') of the NR/CT biocomposites with CT loading from 0 to 8 phr. The increasing temperature has an effect on decreased elastic modulus because high temperature leads to higher molecular movement ability. Although the excellent elastic modulus of the NR/CT biocomposite film increased with chitosan loading, the elongation at break decreased(13).

2.2.4 Reinforcement of Natural Rubber with Bacterial Cellulose via a Latex Aqueous Microdispersion Process

Phomrak et al.(7) developed NR- bacterial cellulose (NRBC) composite films. The mechanical and physical properties of NR composite films were improved by using bacterial cellulose as a reinforcement material in NR. The mechanical properties (Young's modulus, tensile strength, and elongation at break of NR, BC, and NRBC composites) are shown in Table 2 and Figure 9, respectively. The pure NR film has low Young's modulus and low tensile strength but has a high elongation at break.

Conversely, the pure BC has high Young's modulus and high tensile strength but low elongation at break. NRBC composite films have higher tensile and modulus properties than pure NR or BC(7).

The highest Young's modulus and tensile strength are NRBC80 at 4,128.4 and 75.1 MPa, respectively. Due to the increase of crystallinity of BC, it is hard and strong, while pure NR film is soft and tough. However, when the percentage of bacterial cellulose increased, the elongation values of the composite films decreased.

Samples	Crystallinity			Mechanical properties		
	Crystalline area	Amorphous area	Degree of crystallinity* (%)	Modulus (MPa)	Tensile (MPa)	Elongation at break (%)
NR	206	18574	1.10	1.6 ± 0.4	0.8 ± 0.1	111.5 ± 6.4
NRBC20	2267	10391	17.91	244.7 ± 53.5	14.6 ± 3.4	14.6 ± 3.1
NRBC50	2571	5197	33.10	2316.0 ± 303.3	45.9 ± 9.6	6.4 ± 3.2
NRBC80	2479	4352	36.29	4128.4 ± 998.3	75.1 ± 27.1	4.3 ± 1.4
BC	4479	3219	58.18	2288.8 ± 1585.5	54.0 ± 7.6	5.5 ± 2.7

*Degree of crystallinity = crystalline area/total area.

Figure 9 Degree of crystallinity and mechanical properties of NR, BC, and NRBC composites.(7)

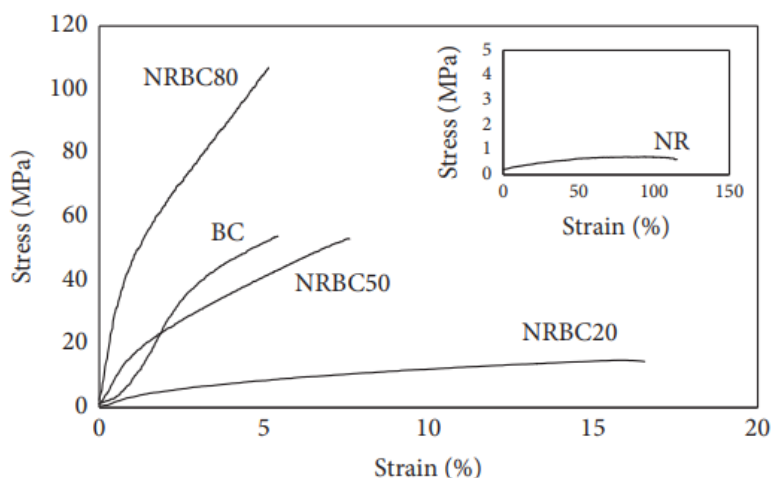


Figure 10. Stress-strain curve of NR, BC, and NRBC composites (7).

2.2.5 Sustainable development of natural rubber and its environmentally friendly composites

Anyaporn Boonmahitthisud (25) presented about sustainable development of natural rubber. She provided up-to-date information on the sustainable development of NR.

Natural rubber (NR) is well known as a renewable biobased polymer that has been widely used in a wide variety of applications because it has attractive properties (toughness, high impact, tear strength, high resilience, and good formation). However, in the rubber industries fillers (especially reinforcing fillers) are necessarily used to

achieve the appropriate characteristics for a variety of commercial applications. The renewable organic fillers derived from natural resources (plant, animal) have advantages including low cost, less abrasive, fewer hazards, and biodegradability. The uses of raw renewable green fillers were sourced from often plant and animal wastes such as wood flour, shrimp and crab shells. The popularities of green fillers are cellulose from plants and chitin or chitosan derived from shrimp and crab shells because they have high strength capacity. In addition, cellulose and chitin are the most abundant natural polysaccharides in the world. Table 3 lists a comparison of reinforcing improvement in NR products with various renewable organic reinforcing fillers.

Table 2. The comparison of reinforcing improvement in NR products with various renewable organic reinforcing fillers (25).

Reinforcing filler	Content	Reinforcing improvement (%) (tensile strength)	Reference
Bamboo cellulosic particle	25 phr	52.4	(27)
Coconut husk cellulosic particles	25 phr	106.5	(27)
Cotton lint cellulosic particles	25 phr	42.2	(27)
Cellulose nanofibers	3 phr	25.9	(28)
Cellulose nanofibers	5 phr	35.4	(29)
Cellulose nanocrystals (one-pot)	10 phr	424.3	(30)
Cellulose nanocrystals (two-pot)	10 phr	345.9	(30)
Cellulose nanocrystals	5 phr	207	(31)
Chitin nanofibers	0.3 wt%	145.3	(32)
Chitin nanocrysta	20 wt%	116.4	(33)

From Table 3, cellulose and chitosan can increase tensile strength. The reinforcing improvement depends on the content in NR product and the process of reinforcing filler adding. She summarizes the several meaningful solutions to achieve the sustainable development of green NR technology.

2.2.6 Electron beam irradiation cross linked chitosan/ natural rubber-latex film: Preparation and characterization.

Chalemchat Sukthawon (34) prepare chitosan/ natural rubber-latex film by electron beam irradiation.

Sulfur vulcanization is a chemical process that converts natural rubber and other polydiene elastomers into cross-linked polymers. The cross-linked elastomers have many improved mechanical properties of natural rubber. The most common vulcanization agent is sulfur. But sulfur vulcanization process is a toxic chemical such as the C-S bond, ZnO, and zinc diethyl dithiocarbamate (ZDEC). These might be dangerous to the environment. The electron beam vulcanization process is an alternative method of vulcanization using electrons to activate free radicals of the carbon in NR to induce chemical reactions in the NR. This technique is environmentally friendly and has no waste.

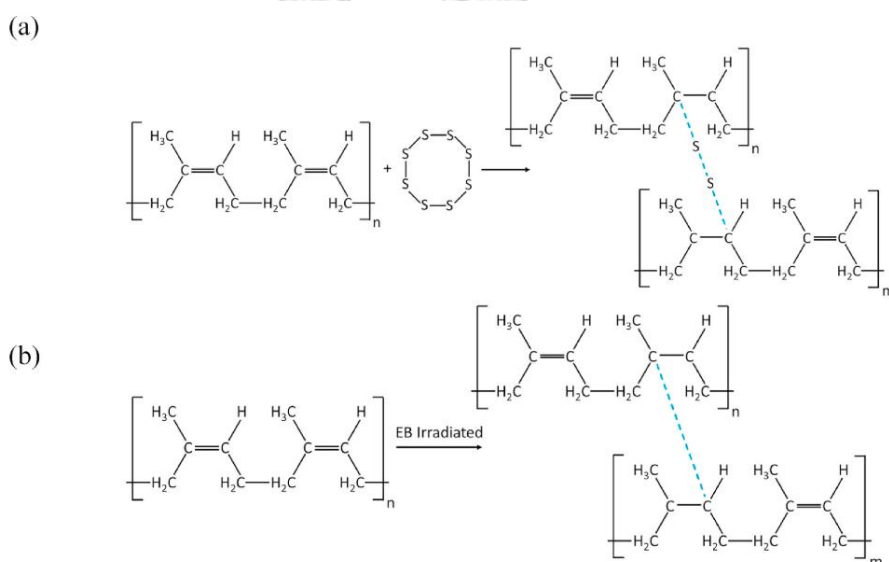


Figure 11. Mechanism of vulcanization of NR (a) sulfur vulcanization (b) EB vulcanization (34).

The CS/NR latex film was prepared at CS loadings of 0–15 phr. The latex compound was vulcanized using the EB vulcanization process at 150–250 kGy and compared with non-vulcanization and sulfur vulcanization. The tensile strength of the CS/NR latex-film at CS loadings of 0,5,10 and 15 phr is shown in Figure 12. The result showed that both the EB vulcanization process and sulfur vulcanization increased tensile strength because of crosslink molecules from vulcanization processes. The highest tensile strength was obtained from the CS/NR latex film at CS loading 5 phr and using the EB vulcanization process at 200 kGy. The maximum tensile strength was obtained at 12.4 MPa. The EB vulcanization of CS/NR latex-film could significantly improve the mechanical properties.

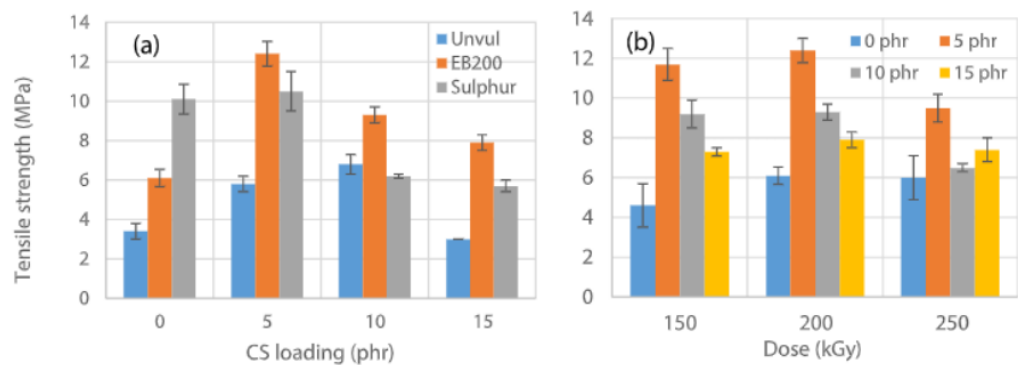


Figure 12. Tensile strength of CS/NR latex-film (a) effect of vulcanization (b) effect of CS loading and radiation dose (34).

2.2.7 A Clean and Sustainable Cellulose-Based Composite Film Reinforced with Waste Plastic Polyethylene Terephthalate

Airong Xu (35) presented methylcellulose (MC) composites reinforced with waste plastics polyethylene terephthalate (PET) with varying the mass ratios of MC and PET. The fabricated MC/PET composites had improved mechanical properties as compared with pure MC. The maximum tensile strength was obtained at 3% PET loading to MC/PET composite (Figure 13). The increase in PET content tended to enhance the elongation at break (Figure 14)

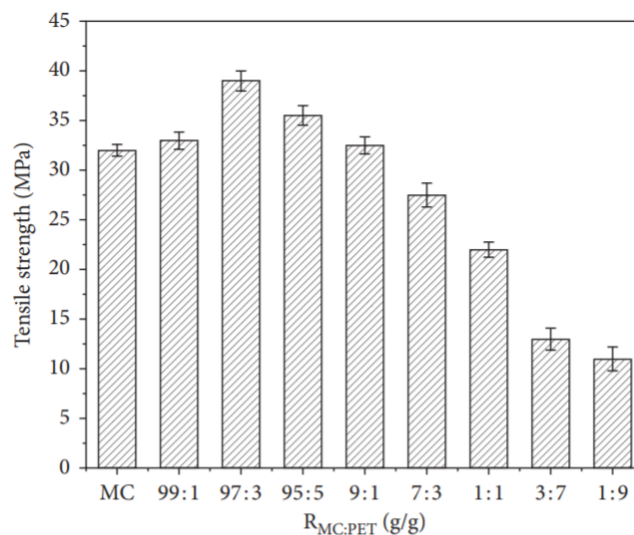


Figure 13. MC/PET mass ratio ($R_{MC:PET}$) dependent on tensile strength of the neat MC film and MC/PET films (35).

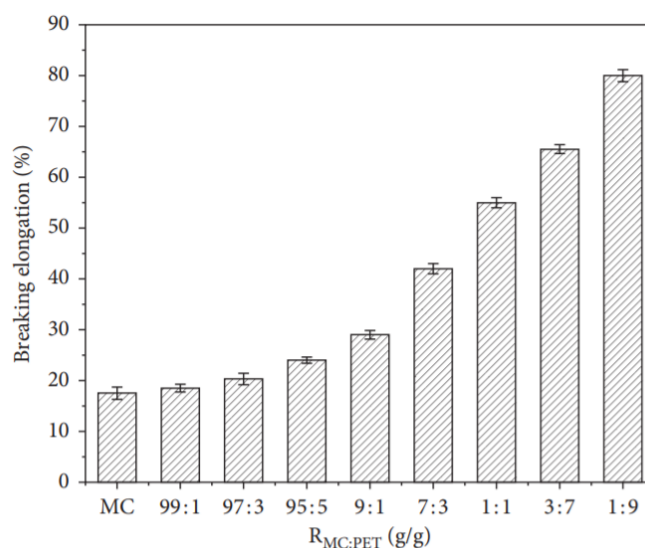


Figure 14 MC/PET mass ratio ($R_{MC:PET}$) dependent on breaking.(35)

2.2.8 A review on mechanical and water absorption properties of polyvinyl alcohol based composites/films

Naman Jain (36) provides an overview of mechanical properties of polyvinyl alcohol (PVA) composite films by a different researchers. PVA is a thermoplastic polymer that is completely biodegradable and nontoxicity. PVA based fiber or particle reinforcing composites shows excellent mechanical. The PVA composite was stronger and tougher than the PVA film because of its good interfacial adhesion. Properties of PVA composite depend on the different blending polymers and the methods of modification. The mechanical properties of different PVA based composites/films are shown in Table 3.

Table 3. Mechanical properties of PVA based composites (36).

Year	Composite/Nanocomposite/Biocomposite	Mechanical properties			Reference
		Tensile strength (MPa)	Elastic modulus (GPa)	Elongation (%)	
2003	Chitosan-PVA (100-0)	55.56 ± 4.65	1.874 ± 0.342	8 ± 2.56	Srinivasa et al. (37)
	Chitosan-PVA (80-20)	46.99 ± 3.85	1.528 ± 0.248	26.84 ± 7.87	
	Chitosan-PVA (60-40)	31.95 ± 6.2	0.539 ± 0.099	28.9 ± 11.7	
	Chitosan-PVA (20-80)	32 ± 5.65	0.231 ± 0.072	70.55 ± 6.9	
	Chitosan-PVA (0-100)	25.64 ± 3.86	0.12 ± 0.056	105.47 ± 6.87	
2011	PVA	14 ± 0.5	0.0447	339.3 ± 0	Zhang et al. (38)
	PVA/cellulose-1	8.8 ± 0.6	0.0963	76.3 ± 7.2	
	PVA/cellulose-5	9.3 ± 0.2	0.0905	118.2 ± 6.2	
	PVA/cellulose-10	10.5 ± 0.6	0.0782	225.9 ± 20.7	

	PVA/cellulose-20	11.6 ± 0.8	0.0703	222.2 ± 22.1	
	PVA/cellulose-30	13.3 ± 1	0.0684	278.3 ± 15	
	PVA/cellulose-40	16.4 ± 0.2	0.0554	374.4 ± 6.4	
2013	Cellulosic film	129.7	0.1297	24.7	Abdulkhani et al. (39)
	Cellulose/PVA film	104.9	0.0469	30.6	

2.2.9 Preparation and properties of natural rubber/chitosan microsphere blends

Ming-zhe (40) prepared the natural rubber/chitosan microsphere blends by ion induction and chemical cross-linking. The natural rubber /chitosan blends showed improved thermal stability, mechanical, hydrophilic, and antimicrobial properties compared with those of natural rubber. The effect of chitosan loadings on mechanical properties of CS/NR blends was investigated. The mechanical properties of natural rubber/chitosan blends with different chitosan microsphere contents are shown in Table 4. Test results confirmed that the tensile strength of the blends increased when the chitosan microsphere content was more than 6 wt%. The effect of chitosan microspheres on the antibacterial properties of natural rubber/chitosan blends presents in Table 5. The antibacterial property of the films was evaluated against *E. coli*. As the result, the inhibitory rate of CS/NR blends increased when the content of chitosan microspheres increased. Therefore, the CS/NR blends had excellent antibacterial properties with chitosan microsphere loadings of 4 – 10 wt% (40).

Table 4. Effect of CS loadings on mechanical properties of CS/NR blends (40).

Property	Chitosan microsphere loading, wt%								
	0	0.50	1.00	1.50	2.00	3.00	4.00	6.00	10.00
Tensile strength, MPa	3.20	3.24	3.37	3.68	4.02	4.18	4.39	5.87	5.61
100% elongation, MPa	0.41	0.41	0.41	0.41	0.42	0.43	0.45	0.49	0.46
300% elongation, MPa	0.49	0.51	0.51	0.51	0.52	0.52	0.53	0.57	0.56
Test strength, kN m ⁻¹	10.85	7.56	8.04	9.35	9.82	10.83	11.06	11.75	12.28

Table 5. Antibacterial properties of chitosan/natural rubber films with different chitosan microsphere loadings (40).

Chitosan microsphere loading (wt%)	Escherichia coli Viable count (cfu ml ⁻¹)	Inhibitory rate (%)
0	309	-
1.00	296	4.21
2.00	186	39.81
4.00	8	97.41
6.00	3	99.03
10.00	0	100.00



CHAPTER III EXPERIMENTAL

3.1 Material

Natural rubber latex (NR) with 60% dry rubber content was purchased from the Rubber Research Institute of Thailand (RRIT, Bangkok, Thailand). Fresh latex is preserved with added chemicals and centrifuged to obtain a concentrated latex of 60% DRC (dry rubber contents). Ammonia is added during the process to enhance the preservation of latex.

The paper sheets of cellulose from eucalyptus pulp were kindly provided by the Teppattana Paper Mill Co., Ltd. (Bangkok, Thailand). The sheets were dried in an oven at 80 °C for 24 h to remove moisture prior to using in the experiment. The microfibrillated cellulose (CE) was prepared by crushing the dried cellulose sheet, grinding by using ball mill (PM 100, Haan, Germany), and sieving, respectively. After grinding, the size of CE particle was in the range of 10–30 µm, with the average particle size of 26.5 µm (evaluated by using Laser particle size distribution (PSD)). Acetic acid 2% (v/v), ammonium hydroxide solution 2.5% (v/v) and other chemical reagents (DI water) were purchased from Sigma-Aldrich (Thailand) Co Ltd. (Bangkok, Thailand).

Chitosan powders (CH) with a deacetylation of 90%, at molecular weight 30,000 g/mol (CHS) and 500,000 g/mol (CHL) were purchased from TS Agritech company (nakhon pathom, Thailand).

3.2 Methods

For the preparation of CE suspension and chitosan solution, The CE suspension was dispersed in deionized (DI) water using ultrasonication at 500 W for 15 min prior to adding in distilled water containing 20 ml of 2% (w/v) of ammonium hydroxide. The chitosan solution was prepared by dissolving chitosan in distilled water containing 20 ml of 2% (v/v) of acetic acid.

To fabricate composite films, 6 g of the natural rubber latex (NR) was slowly added to 20 ml of the CE suspension and 20 ml of chitosan solution. Then the mixture was stirred by high-frequency mechanical stirring until homogenous at room temperature. After that, the films were cast in a plastic tray and dried in an oven at 40 °C for 24 h. The mixtures were prepared for compositions by concentration ratios of CE and CHS/CHL (Table 6). The concentration ratios are expressed as wt. % on a dry rubber contents.

Table 6. The composition of microfibrillated cellulose-chitosan-natural rubber (CE/CH/NR) composite films

SAMPLE	CE (g)	CH (g)		NR (g)
		CHS	CHL	
NR	-	-	-	6
CE5CHS5	0.18	0.18	-	6
CE5CHL5	0.18	-	0.18	6
CE5CHS10	0.18	0.36	-	6
CE5CHL10	0.18	-	0.36	6
CE10CHS5	0.36	0.18	-	6
CE10CHL5	0.36	-	0.18	6
CE10CHS10	0.36	0.36	-	6
CE10CHL10	0.36	-	0.36	6

For Example, The CE5CHS5 was the NR film reinforced by adding in CE suspension 5 wt% and CHS solution of 5 wt%

NR 60% DRC

6 g

Dry Rubber content

$$= \frac{60}{100} \times 6 = 3.6 \text{ g}$$

CE 0.18 g

$$= \frac{0.18}{3.6} \times 100 = 5 \%$$

CHS 0.18 g

$$= \frac{0.18}{3.6} \times 100 = 5 \%$$

3.3 Characterization of physical, biological and chemical properties of the natural rubber films reinforced with cellulose and chitosan

3.3.1 Scanning Electron Microscope and Energy Dispersive X-ray Spectrometer (SEM-EDS)

Surface and cross-sectional morphologies were viewed by Scanning Electron Microscope and Energy Dispersive X-ray Spectrometer (SEM-EDS; JEOL JSM-IT-500HR and JEOL, Japan). The dried NR reinforced cellulose and chitosan films were sputtered with a thin layer of gold in a sputter coater (Balzers-SCD 040, Liechtenstein) and imaged at a magnification of 5,000 and an accelerating voltage of 15 kV.

3.3.2 Fourier Transform Infrared Spectroscopy (FTIR)

The chemical structures of the films were analyzed and recorded by FTIR with a Perkin Elmer, Spectrum One 2 FTIR spectrometer (Bruker, INVENIO®S) at wavenumbers ranging 4000–400 cm^{-1} at a resolution of 4 cm^{-1} .

3.3.3 Mechanical Properties Testing

The maximum tensile strength, Young's modulus, and elongation at break of NR composite films were measured by Universal Testing Machine (Instron, Norwood, MA, USA) following the testing conditions reported in ASTM D882. The average values were determined from at least five specimens and reported as average values with standard deviation (SD).

3.3.4 Thermal Gravimetric Analysis (TGA)

The thermal weight changes of MFC, NR, CH and the films were determined using TGA (Q50 V6.7 Build 203, Universal V4.5A TA Instruments, New Castle, DE, USA) in a nitrogen atmosphere. The scanning range was 30 °C to 700 °C with a heating rate of 10 °C/min. The initial weight of each sample was around 10 mg and percentage weight loss versus decomposition temperature by TGA analysis was determined.

3.3.5 Differential Scanning Calorimetry (DSC)

DSC analysis was used to measure the thermal properties of the films, such as glass transition temperature (T_g) and crystalline melting temperature (T_m). The samples of 4 mg were heated from -100 to 300 °C at a heating rate of 10 °C/min under nitrogen gas. In addition, the curing behavior of the films was determined using a NETZSCH DSC 204 F1 Phoenix (Selb, Germany).

3.3.6 X-Ray Diffraction (XRD)

X-Ray Diffraction (XRD) The examination of the crystal structures of the films was performed by X-ray diffractometer (model D8 Discover, Bruker AXS, Karlsruhe, Germany). The films were cut into strip-shaped specimens of 4 cm in width and 5 cm in length. The operating voltage and current were 40 kV and 40 mA, respectively. Samples were scanned from 5–40° 2 θ using CuK α radiation. Degree of crystallinity (%) of the sample was calculated by the following formula:

$$\text{Degree of crystallinity (\%)} = \frac{\text{Crystalline area} \times 100}{\text{Total Area}}$$

Note.* Calculated by using TOPAS Software (Version 3), Bruker AXS

3.3.7 Contact angle

The dynamic advancing and receding water contact angles under air at room temperature were measured using a contact angle goniometer (Rame-hart, Instrument Co., Succasunna, NJ, USA, model 100-00), equipped with a Gilmont syringe and a 24-gauge flat-tipped needle.

3.3.8 Water Absorption Capacity (WAC)

Water absorption capacity (WAC) was determined by immersing the pre-weight of dry films of 20 mm × 20 mm in DI water at room temperature (30 °C) until equilibrium. Then, the films were removed from water and blotted out with Kim wipes. The weights of the hydrate films were then measured, and the procedure was repeated until there was no further weight change. Water absorption of the sample was calculated by the following formula:

$$\text{WAC (\%)} = \frac{(W_h - W_d) \times 100}{W_d}$$

where W_h and W_d denote the weights of hydrate and dry films, respectively

3.3.9 Toluene Uptake (TU)

Specimens of CE/CH/NR films of 25 mm × 25 mm were weighed and immersed in toluene at room temperature. After that, the specimens were weighed. The procedure was repeated until there was no further weight change. The toluene uptake (TU) was calculated by the following formula:

$$\text{TU (\%)} = \frac{(W_t - W_0) \times 100}{W_0}$$

where W_0 and W_t denote the weights of films before and after the immersion in toluene, respectively.

3.3.10 Antibacterial

The antibacterial of CE/CH/NR composite films against *Escherichia coli* (ATCC 8739) and *Staphylococcus aureus* (ATCC 6538P) were assessed according to the method of JIS Z-2801:2006. The films were cut into 5 cm × 5 cm circular disks, rehydrated in DI water. The incubations of *E. coli* and *S. aureus* occurred at 37°C under aerobic condition for 24 hr. Each microbe was suspended in broth at the standard concentration of 0.4 ml. After the specified time, put the phosphate buffer solution on the film containing the microbial suspension. For elution of microbial suspensions to count the number of microorganisms. Then, the total number of microorganisms inhibition was measured by selecting only concentrations that can count the number of microorganisms between 30-300 colonies.

The percentage reduction was calculated by the following formula:

$$\% \text{ Reduction} = \frac{(B - A) \times 100}{B}$$

A = Log CFU per milliliter of viable microorganisms after treatment (24 hr)

B = Log CFU per milliliter of viable microorganisms before treatment (0 hr)

The antibacterial activity was calculated by the following formula:

$$R = U_t - A_t$$

R = antibacterial activity

U_t = Average of Log CFU per milliliter (Standard) after treatment (24 hr)

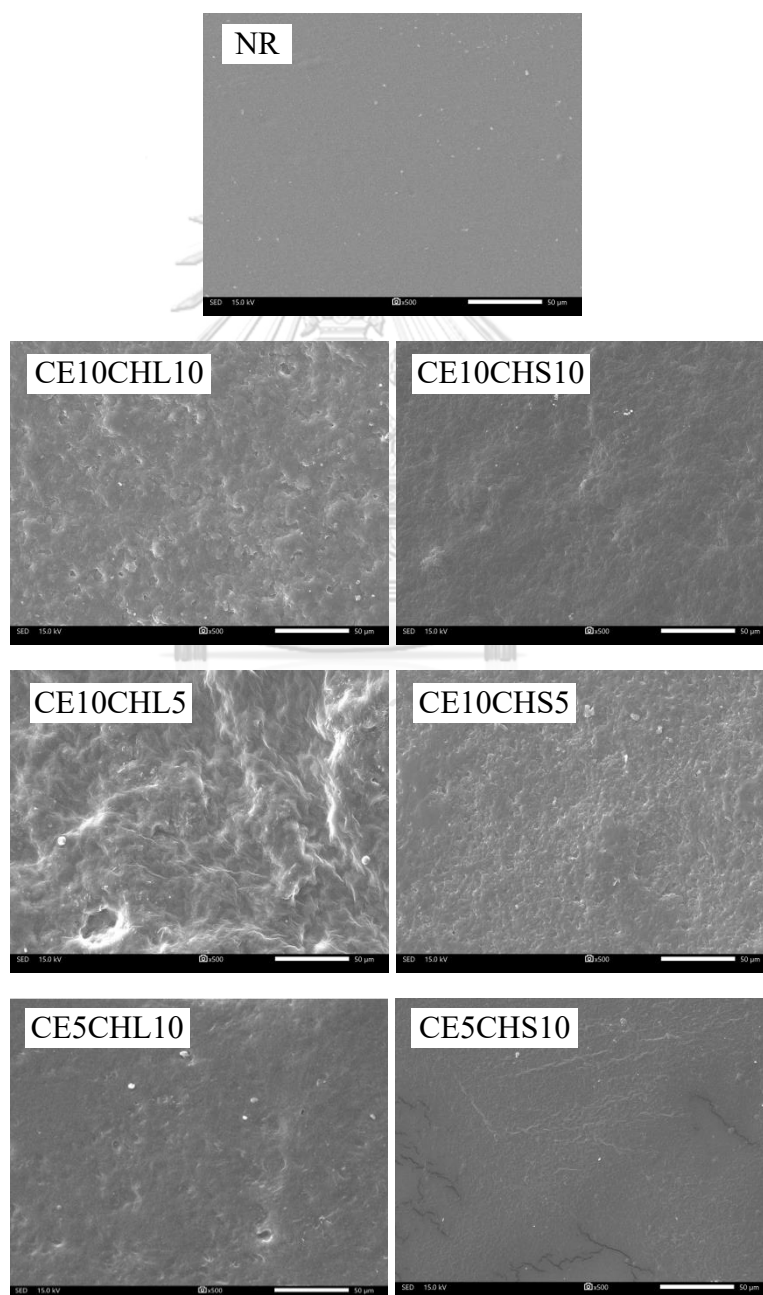
A_t = Average of Log CFU per milliliter (Sample) after treatment (24 hr)

* Antibacterial activity (R) ≥ 2 exhibit to effective in inhibiting microorganisms.

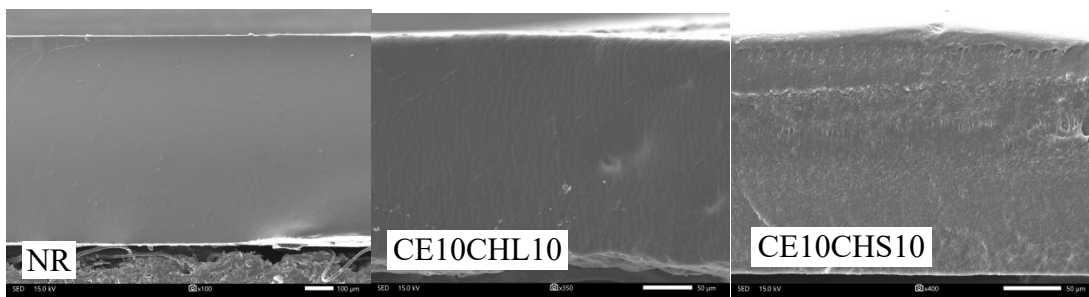
CHAPTER IV RESULTS AND DISCUSSION

4.1 Scanning electron microscopy (SEM)

SEM is known to be one of the best techniques for morphology observations because of its potential in the precise analysis of a solid surface. Figure 15 shows SEM photographs of the surface (a) and the cross-section (b) of the CE/CH/NR films that was prepared by latex aqueous microdispersion. According to the observation, CE and CH were added and mixed homogeneously with NR at the weight ratios of 5-10 wt. % with appropriate CE and CH dispersion and distribution in the NR matrix.



a)



b)

Figure 15. SEM images of the films of NR, CE/CH/NR composites: (a) surface views , (b) cross section views

As observed from Figure 15a, the NR film had a relatively smooth outer surface and homogenous phase compared with those of CE/CH/NR films. The surface of NR film did not have a single pore, whereas the surface of CE/CHS/NR and CE/CHL/NR were rather rougher. CE and CH microfibrils were thoroughly dispersed and interrupted in the rubber matrix as a reinforced filler (16). The surface roughness is caused by the differences in polarity and density of NR, CH and CE (3; 12). The increase in CE and CH concentration could raise the agglomeration of CH and CE in the surface of NR matrix, which led to the higher level of surface roughness and also affect the mechanical properties of films (16).

The films of CE/CH/NR indicate good miscibility between CE and CH on the surface. The higher level of surface roughness of CE/CHL/NR than CE/CHS/NR was observed. For example, CE10CHL5 had a rougher surface as compared to CE10CHS5. This should be because the long chain of chitosan could increase more interactions on the same or neighbor chains (41).

The increase in cellulose content could raise the higher level of surface roughness due to the crystalline of cellulose that added to the amorphous matrix of NR (42). For example, the surface of CE5CHL10 /CE5CHS10 was smoother than CE10CHL10 /CE10CHS10 because of lower cellulose concentration.

In addition, the cross-sectional views demonstrate that the CE and CH particles were well dispersed both at the surfaces and within the NR matrix, without extensive aggregation. Overall, it was shown in this study that the composite films of NR reinforced with CE and CH could be successfully developed by the latex aqueous microdispersion process. However, for the case of high loading of CE and CH, NR matrix might have a possibility to be slightly inconsistent parts. The dehydration and polymerization might also have a significant effect on the surface and cross-sectional morphology structure of CE10CHS10 and CE10CHL10. This reaction may be attributed to strong molecular inter-atomic forces and hydrogen bonding in CE10CHS10 and CE10CHL10. Previously from the study of cellulose/chitosan films, hydrogen bonding was damaged which disrupted the crystalline structures of the

cellulose and chitosan. Therefore, the internal structure became loose and an enhanced surface hydrophobicity was observed (43).

4.2 Fourier-transform infrared spectroscopy (FTIR)

FTIR spectra obtained from NR, CH, CE, and CE/CH/NR are shown in Figure 16. The FTIR spectrum of pure NR shows characteristic peaks at $\sim 2912\text{ cm}^{-1}$, which are assigned to the asymmetric stretching vibration of methylene ($-\text{CH}_2$) and the peak of symmetric stretching vibration of methyl ($-\text{CH}_3$) at 2960 cm^{-1} . The $=\text{C}-\text{H}$ out-of-plane bending is observed at 841 cm^{-1} (44). For pure cellulose, there is a strong broad peak at 3331 cm^{-1} , which is attributed to O-H stretching vibrations from hydroxyl groups. The peak at 2888 cm^{-1} is attributed to the vibration of C-H stretching (45). Moreover, there is a peak of C-O symmetric stretching of primary alcohol at 1026 cm^{-1} . In the case of chitosan, the broad and small peak from 3000 to 3600 cm^{-1} is assigned to N-H symmetric stretching of aliphatic primary amine (46). The peak at 1024 cm^{-1} is attributed to the C-O symmetric stretching of primary alcohol. The FTIR spectra of CHS/NR and CHL/NR composite film show peaks around 3000 – 3500 , 2851 – 2960 , and 841 cm^{-1} , which are assigned to N-H, C-H stretching, and $=\text{C}-\text{H}$ out-of-plane bending, respectively. Therefore, the FTIR results of CHS/NR and CHL/NR composite film confirm the presence of NR and CH. The FTIR results of CE/CHS/NR and CE/CHL/NR composite films also show the consisting of NR, CE, and CH peaks, which were around 2851 – 2960 , 1445 , 1437 and 841 cm^{-1} , assigned to C-H stretching of alkane, $=\text{C}-\text{H}$ stretching vibration of methyl ($-\text{CH}_3$), O-H stretching of alcohol and C-H out-of-plane bending, respectively. The broadband peak at 3000 – 3500 cm^{-1} overlapped by the stretching vibration of the hydroxyl groups and primary amine might imply the intermolecular interaction, occurred between the hydroxyl (OH) and amine (NH) groups of cellulose and chitosan. The position peaks of all composite films display characteristic peaks of CE, CH, and NR.

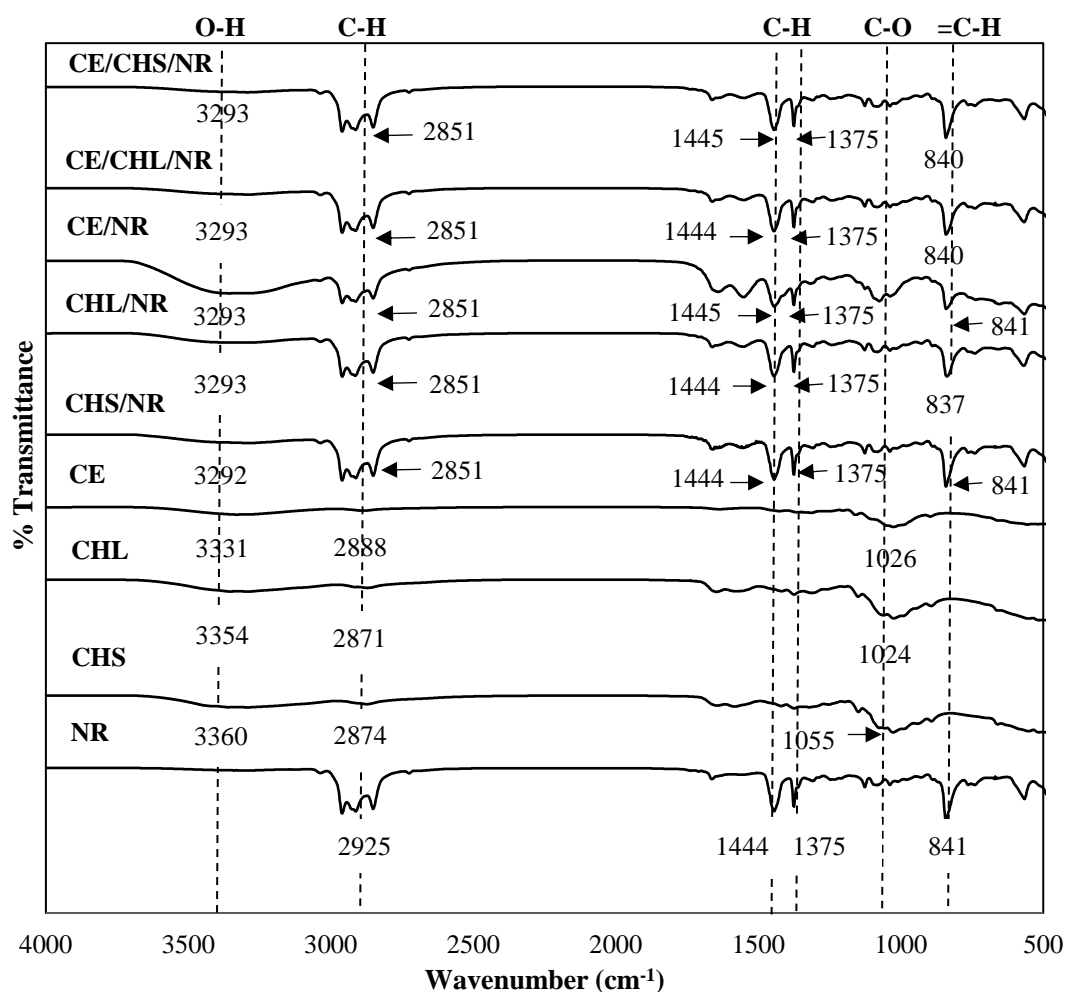


Figure 16. FTIR spectra of NR, CHS, CHL, CE and NR composite films

4.3 Mechanical properties

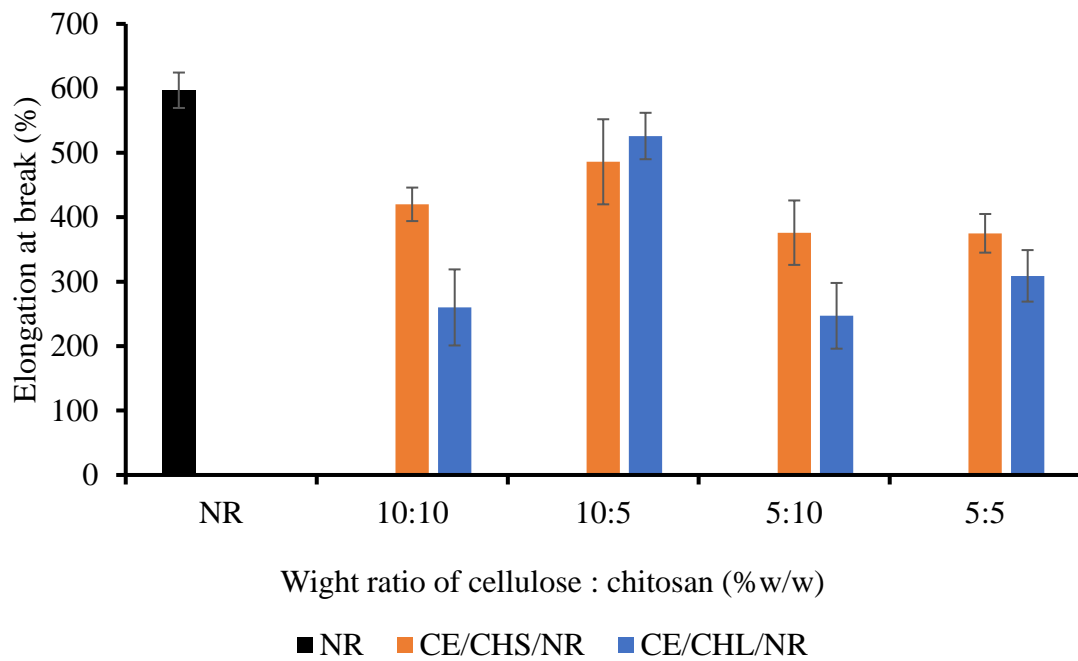
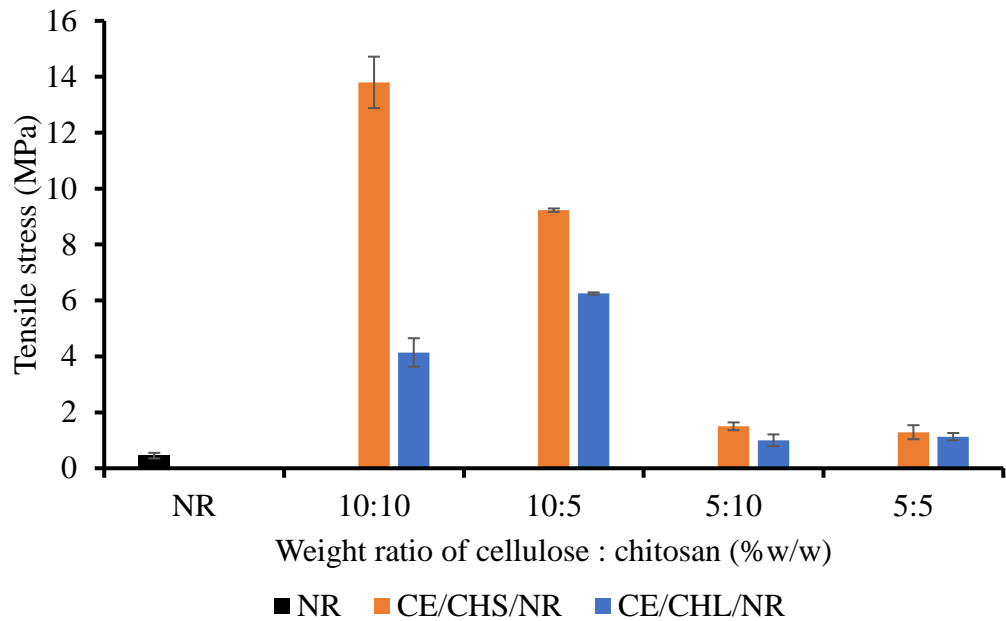
The mechanical properties of CE/CH/NR composite films at the difference ratios of CE and CH. The CE/CH/NR were analyzed in terms of elongation at break, tensile strength, and Young's modulus, as presented in Figure 17. In general, NR is well-known for its high elasticity but low tensile strength (47); while, CE and CH have high tensile strength and Young's modulus (16). Overall, it was shown that CE and CH could be used as reinforcing in the NR matrix. The tensile strength and Young's modulus of the composite films were enhanced with the reinforcement by using CE and CH in a suitable proportion.

The maximum tensile strength (13.8 MPa), Young's modulus (12.74 MPa) was obtained from the composite films reinforced with CE at 10 wt% and CHS at 10 wt%. The incorporation of CE and CH into the NR matrix significantly improved the tensile strength and Young's modulus of the CE10CHS10 (10% w/w of CE and CHS) to 10 times those of the NR film. The good distribution of CE and CH into the NR

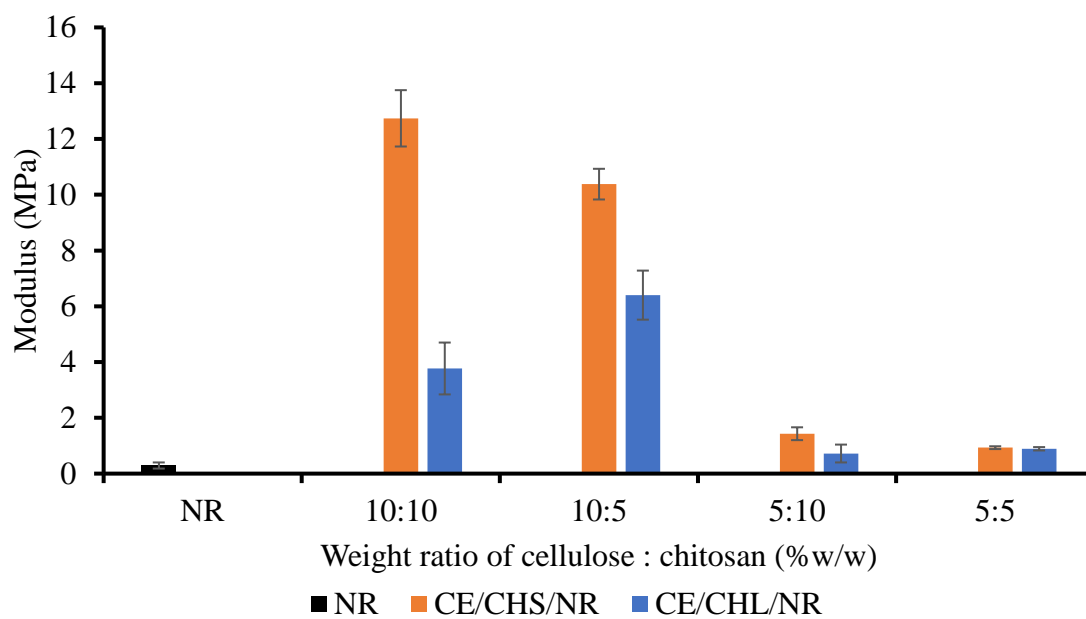
matrix as observed by SEM (Fig. 15) resulted in the reinforcement and improvement of the tensile strength and Young's modulus. Moreover, cellulose and chitosan were thoroughly dispersed, and acted as a reinforced filler (16). This attribute to the fact that a certain amount of cellulose and chitosan cause an increasing in the intermolecular interactions between the hydroxyl group of cellulose, the hydroxyl and amine groups of chitosan (11; 12) for crosslink molecule on hydrocarbon long chains (41). In addition, the tensile strength and modulus of CE/CH/NR composite were increasingly enhanced as compared with NR according to the crystalline of cellulose and chitosan being added into the amorphous matrix of NR (48).

CHL could form interactions of hydrogen bonding with CF better as compared to CHS (49). Therefore, the suitable weight ratio of CE: CHS was 1:1, which less than the CE: CHL (2:1). The film of CE10CHS10 had greatest tensile stress and modulus among CE/CH/CHS composites. Whereas, the film of CE10CHL5 had greatest tensile stress and modulus among CE/CH/CHL composites.

A significant reduction in the elasticity of NR composites reinforced with CE and CH was examined by the decrease in elongation at the break of CE/CH/NR composite films (Fig. 17b). It can be observed that CE10CHS10 (420%) and CE10CHL10 (260%) have lower elongation than CE10CHS5 (486%) and CE10CHL5 (526%) due to the increasing of cellulose and chitosan concentration. When the percentage of chitosan increases, the chain flexibility of the system was greatly limited (13) and the molecular mobility of natural rubber was reduced (25). The interaction of hydrogen bonding from cellulose and chitosan could cause the formation of a rigid three-dimensional network in the natural rubber matrix. Then, NR chains obstruct the mobility. Furthermore, the higher percent of CE and CH significantly reduced the elasticity of the composite films as compared to the NR film. However, the elongation of the composite films of CE/CH/NR was much higher as previously observed from CE/NR composites (7).



b)



c)
Figure 17. a) Tensile strength b) Elongation at break c) Modulus of composite films as a function of the weight ratio of cellulose and chitosan in NR composites.

4.4 Thermal Gravimetric Analysis (TGA)

The thermal degradation was determined by using thermogravimetric analysis (TGA) and derivative thermogravimetry (DTG). The TGA curves show percent weight loss of CE, NR, CH, and CE/CH/NR composite films at different heating rates in nitrogen atmosphere are presented in Fig. 18. The shapes of TGA curves are quite similar shifting toward higher temperatures at higher heating rates (50). This is due to the heat transfer lag with an increased heating rate. The parameters were calculated from TGA and DTG thermograms of samples at a heating rate of $10^{\circ}\text{C min}^{-1}$ in a nitrogen atmosphere.

The slight weight loss at a temperature below 200°C is associated with the vaporization of volatile components such as moisture or solvent. The peak of water evaporation from cellulose (CE) appeared around 59°C , which was 10% of the initial weight. On heating below 200°C , the degradation of polymers indicates cross-link breakage (51). The polymer degradation into gaseous products was observed. Then, the heating removes all organic matter and leaves a residue of inorganic fillers in the composites (17).

The TGA curves present single-step thermal decomposition of NR, CH, and CE films in the ranges of $340\text{--}470^{\circ}\text{C}$, $250\text{--}320^{\circ}\text{C}$, and $260\text{--}380^{\circ}\text{C}$, respectively. The NR film demonstrated better thermal-resistant performance than CE and CH film. The percentage weight loss of pure CE across a temperature range of $210\text{--}240^{\circ}\text{C}$ is ~ 5.8 wt.%, indicating the decomposition of proteins (52). Moreover, a result in a residual char product (≈ 20 wt.%) occurs at a temperature range of $300\text{--}360^{\circ}\text{C}$. The CE/CH/NR composites films showed peaks of the polymer decomposition, similar to those of NR. At a temperature below 200°C , the weight loss is associated with the vaporization of water. The TGA total weight loss was about 99% for NR film, 51–54% for CH films, and 80% for CE film. Similar patterns of TGA curves of NR, CH and CE films were previously reported (7; 13).

For the composite films, the thermal degradation of CE/CH/NR films in the first step with an initial decomposition of 340°C , which was close to that of NR film. The total weight losses of the composite films were in the range of 93–98%, depending on the concentration of cellulose and chitosan contained in the film. The total weight loss of the composite film containing the highest cellulose and chitosan (CE10CHS10 and CE10CHL10) was about 93% and 95%, respectively.

The maximum rate of weight loss in the composite films occurs at $300\text{--}450^{\circ}\text{C}$ by the decomposition of CE, CH, and NR, respectively. At temperatures above 450°C , the remained remaining weight of the decomposition products such as char, the non-volatile residual with high carbon content. The char yield of CE10CHS10, CE10CHL10, CE10CHS5, CE10CHL5, CE5CHS10, CE5CHL10 were 7.65%, 4.81, 5.13%, 1.57%, 3.77%, and 1.10%, respectively. The residual quantities of the CE/CH/NR composites films slightly increase as the chitosan and cellulose content increases in the NR matrix. Which is explained by the interaction between the hydroxyl groups of the cellulose and the amino groups of the chitosan (53). It was observed at the maximum degradation rate. This phenomenon may be mainly attributed to the similar chemical structure of cellulose and chitosan. Between chitosan with different MW, the CE10CHL10 has a lower char yield than

CE10CHS10; because CHL has a vast carbon atom in the chain compared with CHS (49).

The CE/CH/NR composites films presented slightly increased thermal stability when compared with CE and CH. The thermal stability of total composite films is similar to the NR, which corresponds to great distribution and dispersion of CE and CH in the NR matrix. The interfacial adhesion between fibers and NR matrix could be enhanced resulting in more interaction between CE, CH, and NR. From the study, It can be confirmed that the composite films of NR were reinforced with CE and CH by the latex aqueous microdispersion process.

The DTG curves show the percent derivative weight of CE, NR, CH, and CE/CH/NR composite films at different heating rates in the nitrogen atmosphere as shown in Fig. 19. Under the thermal analysis, all samples showed main degradation stages at 200–600 °C, and hydrocarbon compounds could efficiently shift the process to lower temperatures with lower maximum weight loss rate (MWLR) and more residues. The decomposition of NR and CE/CH/NR composite films occurs in a single step as confirmed by DTG curves.

The decomposition of CE, CHS, and CHL occurs in two steps as confirmed by DTG curves. At the initial step, the percent derivative weight of CE, CHS, and CHL are around 2%/min at a temperature of approximately 100 °C, which is associated with the vaporization of volatile components such as moisture or solvent. In the 2nd step, the main decomposition of CHS and CHL occurs around 297.4 °C and 293.3 °C, respectively, which is assigned to depolymerization reaction. On the other hand, the DTG maxima temperature in case of CE and NR occurs at 351.4 °C and 379.5°C, which is quite higher than that of chitosan. This indicates that the amino polymer is less thermally stable than the hydrocarbon polymer (43).

The parameter maximum weight loss rate (MWLR) for NR is highest (18 % min⁻¹), then cellulose (14 % min⁻¹), and chitosan (8-9 % min⁻¹), respectively. Also, MWLR for CE/CH/NR composites lies in between those of NR, cellulose, and chitosan i.e. 14.5 % min⁻¹. It means that the CE/CH/NR composites contain mostly NR with some dispersion of cellulose and chitosan, which corresponds to the internal components of the composite films.

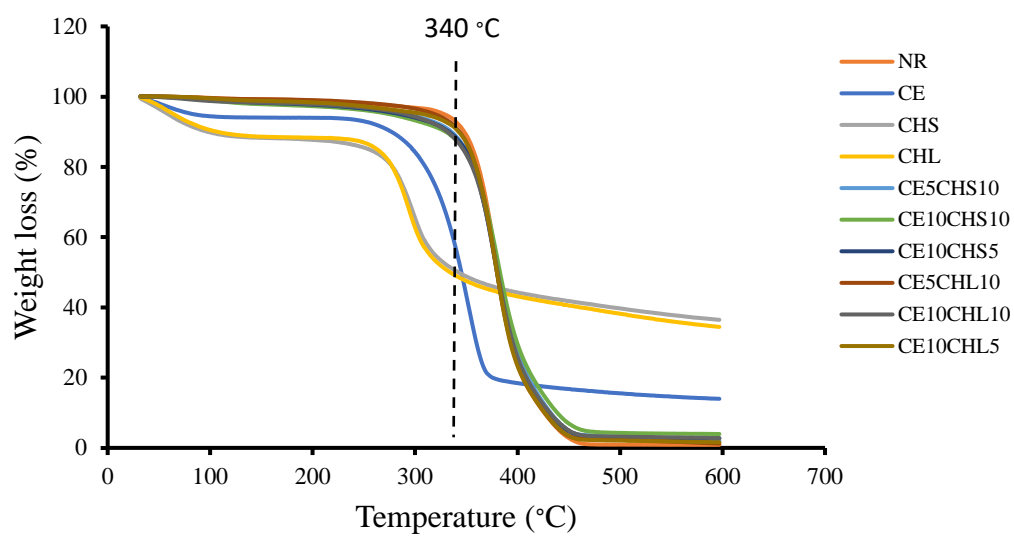


Figure 18 Thermal gravimetric analysis (TGA) curves of NR, CE, CH and CE/CH/NR composite films.

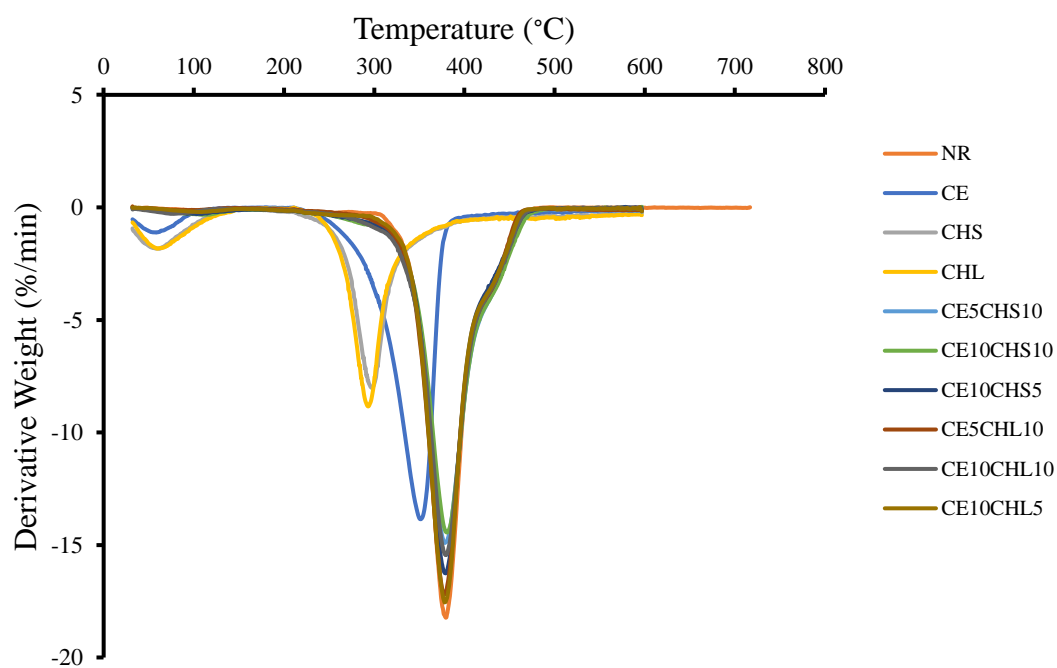


Figure 19 Derivative Thermogravimetry (DTG) curves of NR, CE, CH and CE/CH/NR composite films.

4.5 Differential scanning calorimetry (DSC)

Differential Scanning Calorimetry is widely used to measure thermal analysis techniques in which the heat flow into or out of a sample is measured as a function of temperature and time, while the sample is exposed to a controlled temperature program. DSC analysis provides glass transition temperature, melting, crystallization, specific heat capacity, and thermal stability of polymers in different conditions. In this study, the DSC chromatograms of dried NR, CE, and CE/CH/NR composites films performed -100 to 300°C at a heating rate of $10^{\circ}\text{C min}^{-1}$ under nitrogen atmosphere are given in Figure 20.

The thermogram corresponding to NR film revealed its amorphous nature, with the glass temperature of -64.2 to -61.3°C . The NR has very low glass transition temperature ($T_g \sim -65^{\circ}\text{C}$). The physical and mechanical properties of the film are dependent on the extent of natural rubber latex particles, which are able to coalesce and fuse into each other (54).

The reinforcement by adding CE and CH with a weight ratio of 5-10 wt.% caused a slightly higher T_g . For the composite films, the range of T_g was similar (-61.3 to -62.6°C) regardless of the different compositions of CE, CH, and NR. Generally, the value of T_g depends on the mobility of the polymer chain (55). A lower T_g of composite films indicates higher polymer flexibility or mobility. The main relaxation phenomenon associated with the inelastic manifestation of glass transition was observed from the sharp decrease in temperature. According to the thermograms of all the composite films, no significant change in T_g was observed. Previously, the change in glass transition temperature of NR compounding with cellulose and chitosan has also been found to be negligible (7). Therefore, the reinforcement by adding CE and CH into the NR matrix did not significantly affect the T_g .

According to Figure 20 (b), DSC chromatograms under the first heating scan from 0 to 300°C of CE, CHS, and CHL showed peak T_m values at 107.2 , 134.7 , and 140.1°C , respectively. Generally, T_m depends on the molecular weight of the polymer and thermal history (56). In case of CH, the T_m of CHS (MW 30,000) was less than CHL (MW 500,000) due to the molecular weight less than CHL. The T_m of the composite is higher when compares with pure NR because CE and CH might cause the disorder and disarrangement of NR. The inter-molecular hydrogen bonds create the adding CE and CH in the NR matrix was found to enhance the stability of structure composites (43).

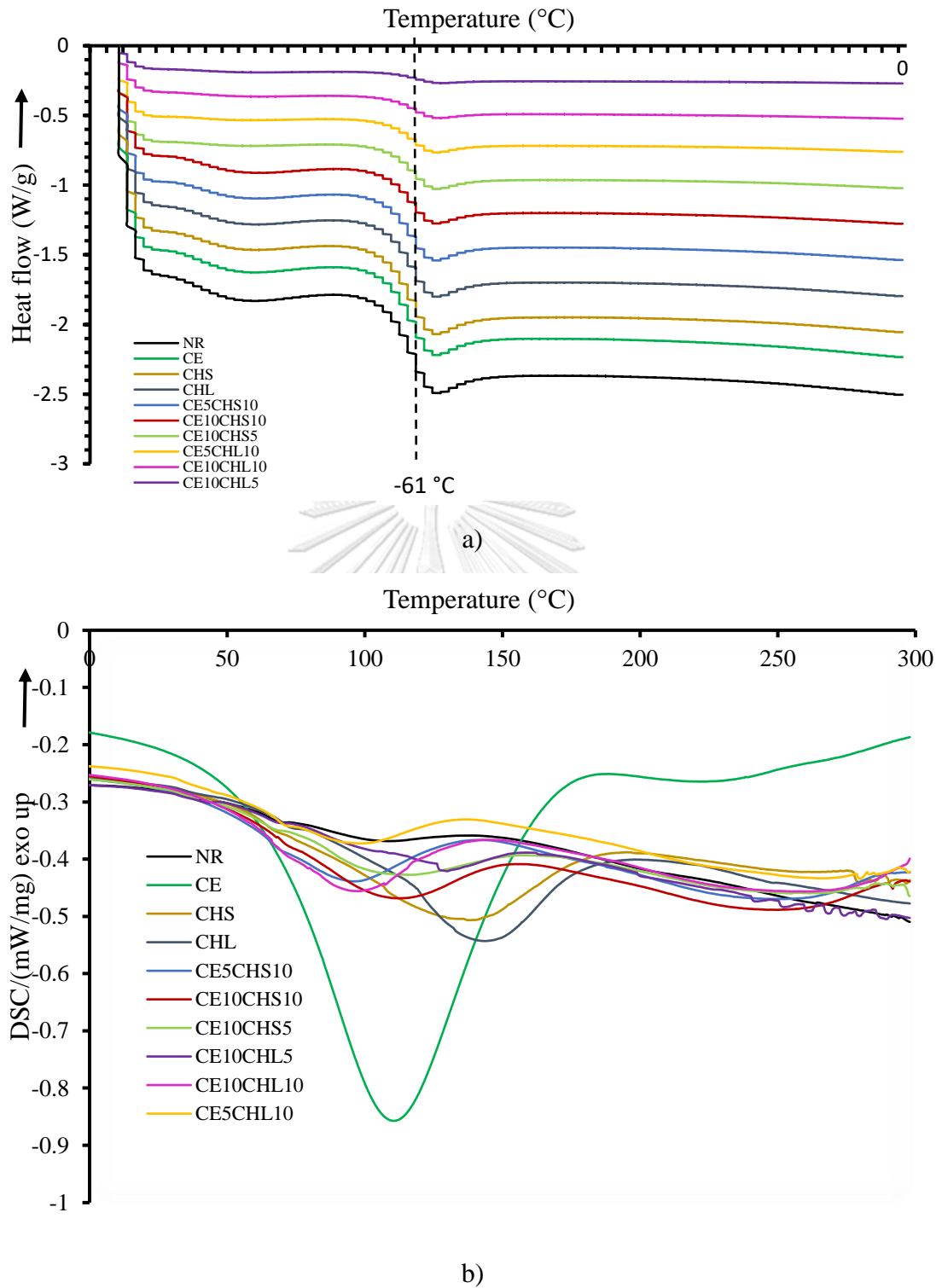


Figure 20 DSC chromatograms of NR, CE, CH and CE/CH/NR composites.

4.6 X-Ray Diffraction (XRD)

The material crystallinity was determined by XRD analysis. In order to better confirm the existence of interaction between CE, CH, and NR. The XRD patterns of NR, CE, CHS, CHL, and CE/CH/NR composite films are shown in Figure 21 and Table 7. The crystalline and amorphous curves, along with the crystallite sizes and the calculation of the degree of crystallinity are shown in Table 8.

The characteristic peaks of CE comprise three main peaks at two theta angles of 16.3°, 22.3°, and 34.6°. The diffraction peaks of CE were sharp and highly dense, associated with the typical profile of cellulose (42). The XRD pattern of CH shows characteristic peaks at a two-theta angle of 9.9°, 19.8°, and 21.5°. The former peak is corresponded to the hydrated crystalline structure of CS, while the peak at 21° is due to the amorphous state of CS (57; 58). The NR film displays a typical diffraction pattern of an amorphous polymer having a significant broad peak located at a two-theta angle of 18.3°(4).

The CE10CHS10 and CE10CHL10 have demonstrated the same characteristics of the NR film diffraction pattern, indicating a less crystalline material or amorphous material. The peaks at a two-theta angle of 18° became slightly more intense, which might imply that the integration of CE and CH into NR might have some effect on the amorphous structure of NR. It could also be noticed that the diffraction peak of CE and CH cannot be observed in the profiles of the composites. This could be due to the cellulose and chitosan being well dispersed in NR.

The NR, CE, CHS, and CHL had crystallinity values at 0%, 62%, 76%, and 63%, respectively. (Table 8) The degree of crystallinity of CE10CHL10 film was 0.72%, whereas the crystallinity of CE10CHS10 film dropped slightly to 0%, which might be more likely due to the relatively less uniform CE and CHS distribution. The loss of crystalline nature of cellulose in the composite films was previously suggested by hydrogen bonding between NR and CE, which allows some parallel chain arrangement in the crystals of cellulose (51). As the result, the CE10CHS10 and CE10CHL10 were a low percent of crystallinity as pure NR. According to the mechanical properties result in Fig. 17, CE10CHS10 and CE10CHL10 had high elongation closely to the NR.

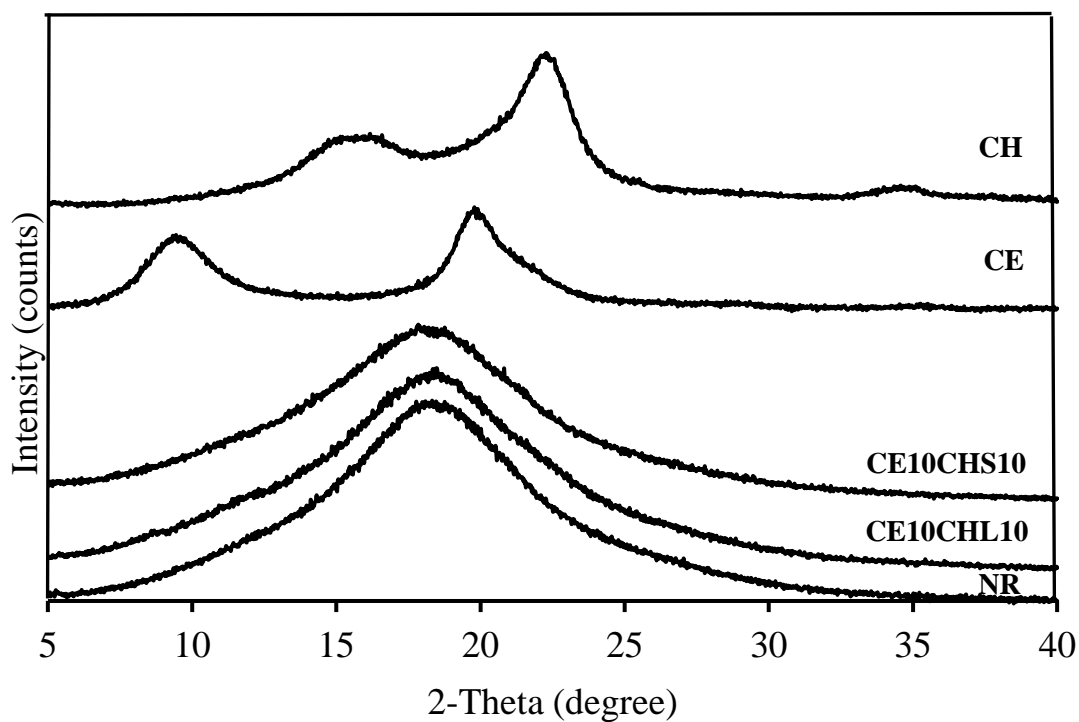


Figure 21 X-ray diffraction (XRD) patterns of CE, CH, and CE/CH/NR films.

Table 7. The crystallite sizes of NR and NR composite films.

Samples	Position (2Th degree)	Crystallite Size (nm)
NR film	5.2744	82.6
	11.9670	1.1
	18.3423	1.1
	25.8283	1.2
CE	15.0814	2.7
	18.1325	0.9
	16.3873	8.2
	20.5772	4.5
	22.2738	4.7
	34.6167	4.7

Samples	Position (2Th degree)	Crystallite Size (nm)
CHL	9.4920	3.0
	14.7791	0.4
	19.7616	5.3
	21.4644	4.1
CHS	9.9067	3.7
	15.0413	0.4
	19.7277	6.3
	21.7592	4.3
	29.3387	10.4
CE10CHL10	9.8126	104.7
	11.4187	1.0
	18.1250	1.6
CE10CHS10	11.6761	1.3
	18.3122	1.1
	23.9011	0.8

Table 8 Calculation of degree of crystallinity

Sample	NR	CE	CHL	CHS	CE10CHL10	CE10CHS10
Crystalline area	19.7	18722.7	16192.4	21215.7	38.8	0
Amorphous area	69512.2	11260.3	9311.4	6551.5	56620.4	68025.8
Crystallinity (%)	0.03	62.44	63.49	76.41	0.07	0











Note.* Calculated by using TOPAS Software (Version 3), Bruker AXS

$$\text{Degree of crystallinity (\%)} = \frac{\text{Crystalline area} \times 100}{\text{Total Area}}$$

4.7 Contact angle

The material hydrophilicity was determined by measuring the contact angle of the films. A contact angle is formed when a drop of liquid is placed on a material surface and the drop forms a dome shape on the surface. The contact angles of pure NR, CE, CHL, and CHS films were around 102.2, 74.5, 94.8, and 91.2, respectively (Table 9). Generally, NR is a hydrophobic substance owing to a long chain of hydrocarbon polymer (59). Thus, it does not perform well when exposed to oils and hydrocarbon solvents, as a result of its nonpolar character (60). In this study, the improved products from natural rubber have potentially wide applications as a result of reinforcing by cellulose and chitosan. In addition, the material hydrophilicity increased with the increase in the polarity of the CE/CH/NR composites from a high polar function such as hydroxyl, amine of reinforcing agents. The dynamic contact angle of the NR was decreased with the addition of CE and CH. The increase in the number of surface hydroxyl groups by the addition of CH and CH enhanced the hydrophilicity of the films. Besides, the contact angle could be decreased because of the roughness surface (61). The contact angles of the composite films of CE10CHS10 and CE10CHL10 were around 88.3 and 82.3, respectively. Because cellulose and chitosan had a vast amount of hydroxyl groups, the NR composite films which contained a high amount of CE and CH showed enhanced hydrophilicity. Therefore, the reinforcement would affect water absorption capacity and solubility in polar and nonpolar solvents, which should be examined for further application.

Table 9. Degree of dynamic water contact angles (°) of NR, CE, CHL, CHS and CE/CH/NR composites.

NR	CE	CHL	CHS	CE10CHS5	CE10CHL5	CE10CHS10	CE10CHL10	CE5CHS10	CE5CHL10
102.2 ± 1.2	74.5 ± 1.8	94.8 ± 2.8	91.2 ± 4.7	96.8 ± 4.7	95.7 ± 4.7	88.3 ± 6.4	82.3 ± 3.0	94.2 ± 2.6	95.2 ± 5.1
									

4.8 Water Absorption Capacity (WAC)

Water absorption capacities of NR and CE/CH/NR films were carried out for 0–150 min of the immersion time (Figure 22). It was demonstrated that the reinforcement of CE and CH at 5-10%wt. in the NR matrix enhanced the rate of water absorption. During 30 min of immersion, water was rapidly absorbed into CE10CHS10, CE10CHL10, CE10CHS5, CE10CHL5, CE5CHS10, and CE5CHL10 films, whereas the pure NR films slowly absorbed water until concentrations reached equilibrium at around 150 min because a long chain of hydrocarbon polymer of NR enhanced hydrophobic property (60). The WAC of the composite films increased with an increase in CE and CH content since cellulose and chitosan are highly hydrophilic and able to form hydrogen bonding to water. According to the chemical structure of cellulose and chitosan, the cellulose and chitosan content in the composites increased the amount of hydrogen bonding due to hydroxyl and amine functional groups (62).

The WAC of the CE/CH/NR composite films were non-linearly increased with CE and CH loading content. The WAC values of NR films were less than 10% of the dry weight, whereas those of the other composite films were 30–60%. Overall, The CE10CHS10 and CE10CHL10 have high water adsorption at 56% and 58%, respectively. The CE10CHL10 has more water absorption capacity than CE10CHS10 since CHL could form a vast number of hydroxyl groups compared to CHS(46), For example the WAC of CE5CHL10 (27%) was higher as compared to that of CE5CHS10 (14%).

The WAC of CE10CHL10 (58%) was higher than that of CE10CHL5 (40%) and CE5CHL10 (34%) because the percent of WAC increased with increasing CE and CH content since the abundant interaction between water and the hydroxyl group in the chemical structure of cellulose and chitosan enhanced hydrophilic property of the films (62). Moreover, the increasing concentration of cellulose was found to have a greater influence on WAC than chitosan. This can be explained by the difference in the WAC between CE and CH by their respective porous structure. Water molecules were thought to be physically trapped by the delicate network structure of cellulose. The incorporation of chitosan may make the surface more compact with smaller porosity, which reduced the water uptake (63).

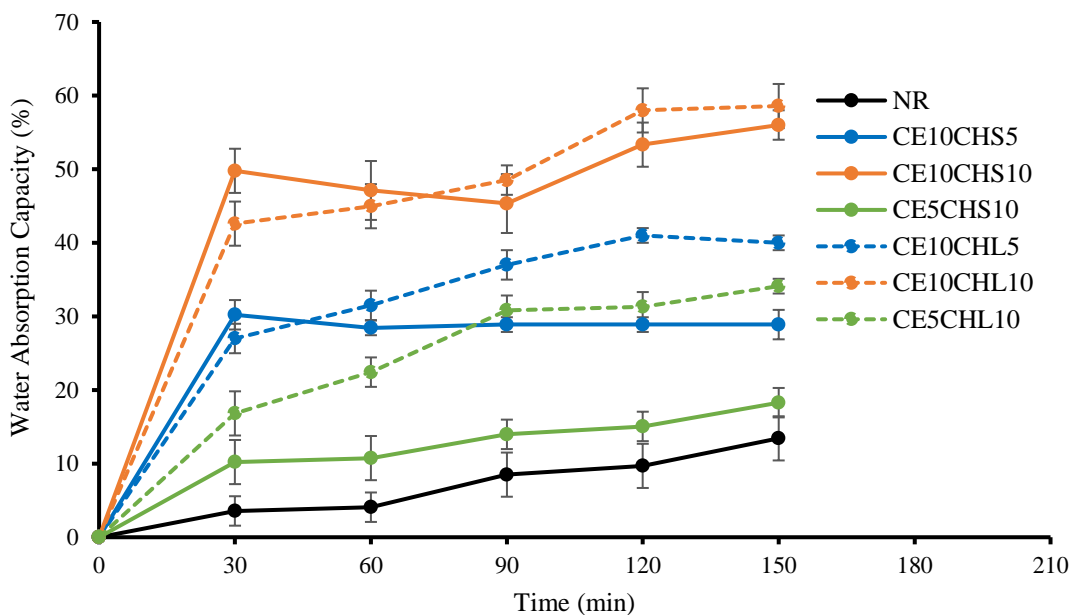


Figure 22 Water absorption capacity (WAC %) with time of NR and CE/CH/NR composite films

4.9 Toluene Uptake (TU)

Toluene uptake of NR and CE/CH/NR films were carried out with respect to the immersion time of 0–150 min (Figure 23). The reinforcement of CE and CH at 5–10% wt. in the NR matrix enhanced the hydrophilic property of the films. NR is a nonpolar polymer owing to a long chain of hydrocarbon polymer (60). Therefore, it is soluble in a non-polar solvent. Toluene is an aromatic solvent that is mainly used in many rubber industries. In this study, the effect of toluene uptake on NR and CE/CH/NR composite films were investigated.

During the initial stage, the floating of the NR film and the composite films were observed. The swelling behavior in toluene of NR film was detected within 90 min, and then the toluene uptake of the NR film rapidly increased and reached the maximum value at 450% in 150 min. At low loading content of CE and CH of 5% and 10% (CE5CHS10, CE5CHL10), rapid toluene uptake rate (150–200% toluene uptake) was noticed during the first 30 min, but the composite films with CE and CH loading content of 10% and 10% (CE10CHS10, CE10CHL10) showed excellent solvent resistance with only 12% toluene uptake after 150 min. No considerable structural change of the CE10CHS10 and CE10CHL10 films were observed during immersion in toluene for 150 min. The toluene uptake of CE/CH/NR composite films decreased with adding CE and CH in the NR matrix due to the chemical structure of cellulose and chitosan. The increase in hydroxyl and amine groups with increasing CE and CH content enhanced the hydrophilic property of the composite films (62).

The integration of CE and CH into the NR matrix promoted the toluene resistance of the CE/CH/NR films. Because toluene is a nonpolar solvent, it can easily

diffuse into NR matrix and cause NR films to swell. If NR is in toluene for a sufficient amount of time, it will dissolve. However, toluene does not dissolve cellulose and chitosan, which is a polar compound. The increased CE and CH incorporation into the NR matrix yielded tight interlocking to obstruct the toluene permeability (64).

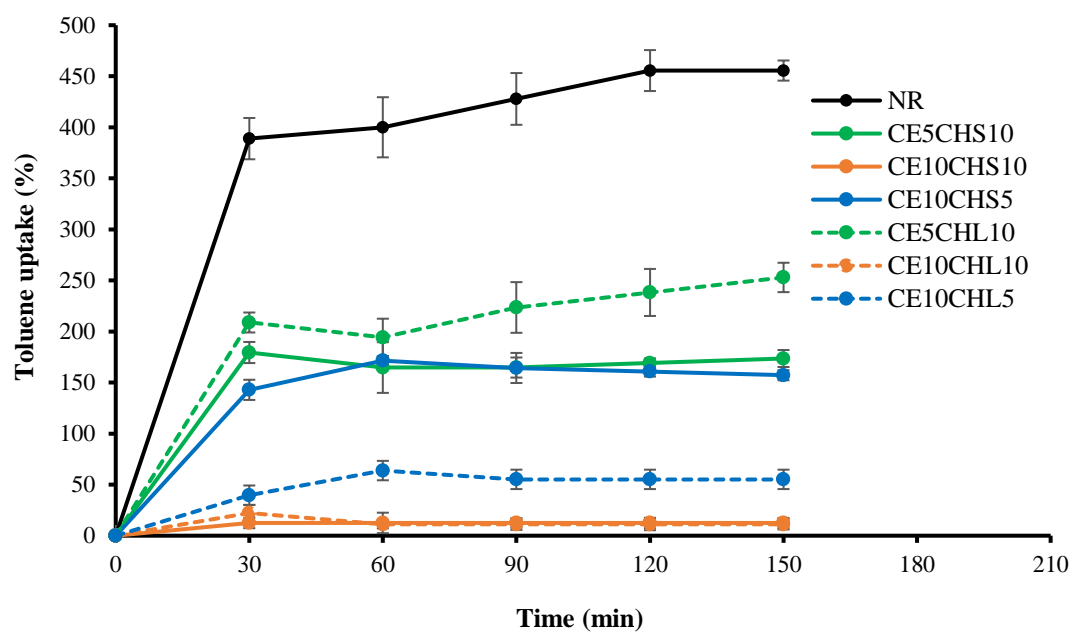


Figure 23 Toluene uptake with time of NR and CE/CH/NR composite films

4.10 Antibacterial ability

Escherichia coli (*E. coli*) and *Staphylococcus aureus* (*S. aureus*) were used for the antibacterial tests of the NR and CE/CH/NR films. The reinforcement of CE and CH at 5-10%wt. in the NR matrix enhanced the antibacterial ability of the films. Generally, chitosan can effectively control the growth and reproduction of hazardous bacteria and also control toxic (16). The antibacterial activity of chitosan was greater on *E. coli* than *S. aureus* cells regardless of the times and temperature (65). The incorporation of chitosan was expected to decrease the bacterial growth on CE/CH/NR composites films. The antibacterial properties of NR and CE/CH/NR composites were evaluated by direct contact with *E. coli* or *S. aureus* for 24 h.

The results as shown in Table 10 and Figure 24-25, The maximum antibacterial activity (R) at 4.56 against *S. aureus*) and 4.83 against *E. coli*) was obtained from the composite films reinforced with CE at 10 wt% and CHS at 10 wt% (CE10CHS10). The CE/CH/NR composite films demonstrated remarkable bacterial inhibition against Gram-negative (*E. coli*) and Gram-positive (*S. aureus*). These results also revealed that the addition of chitosan in CE/CH/NR composite films significantly increased the antibacterial efficiency. The antibacterial activity of chitosan is divided into two proposed mechanisms, both of which are related to the number of active amino groups (66). In one mechanism, the positively charged chitosan would interact with the negatively charged bacteria surface and cell growth inhibition. Another mechanism is that binding of chitosan with DNA may inhibit the mRNA generation of bacteria. In the case of CE10CHS10, the reduction in viable counts was 100% for *E. coli* and 99% for *S. aureus*).

In the study, CHS can inhibit microorganisms more effectively than CHL. The percentage of reduction increased with increasing CH content because CHS has more the amount of active amino groups compared with CHL (66). Previously, it was reported that the CH/NR composite with the chitosan microspheres content of 4 – 10 wt% had excellent antibacterial properties (43). However, not only the concentration of chitosan in the NR matrix, the antibacterial ability of composite films composed of chitosan should also depend on their cationic nature, molecular size (67). Moreover, the antibacterial activity depended on polymeric molecular weight (MW) and degree of acetylation (DA) and also varied according to microorganism strains (68).

Therefore, the concentration and molecular weight (MW) of chitosan would clearly affect antibacterial activity (R) and the percentage reduction (% Reduction) of *E. coli* and *S. aureus*.

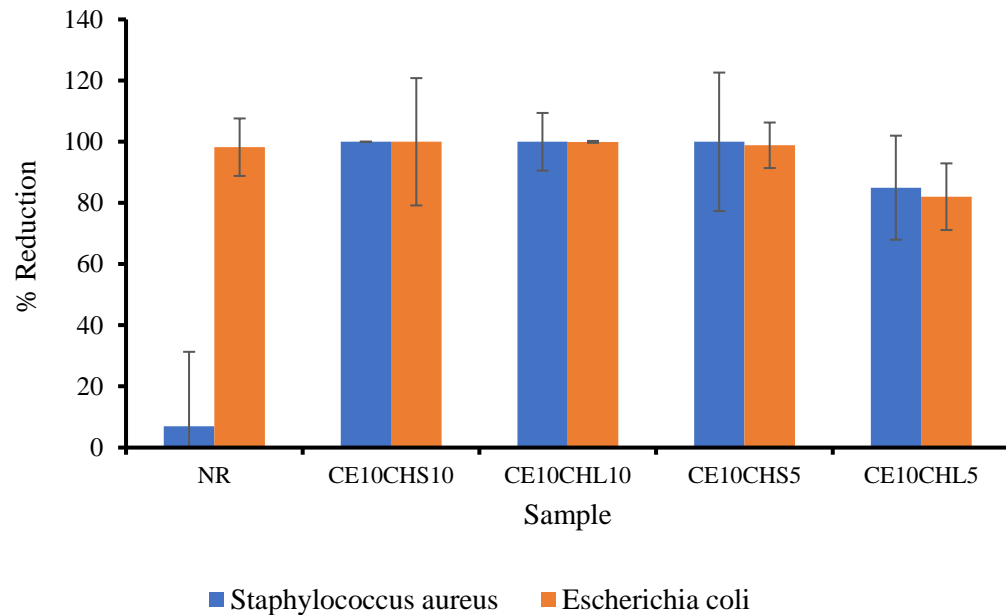
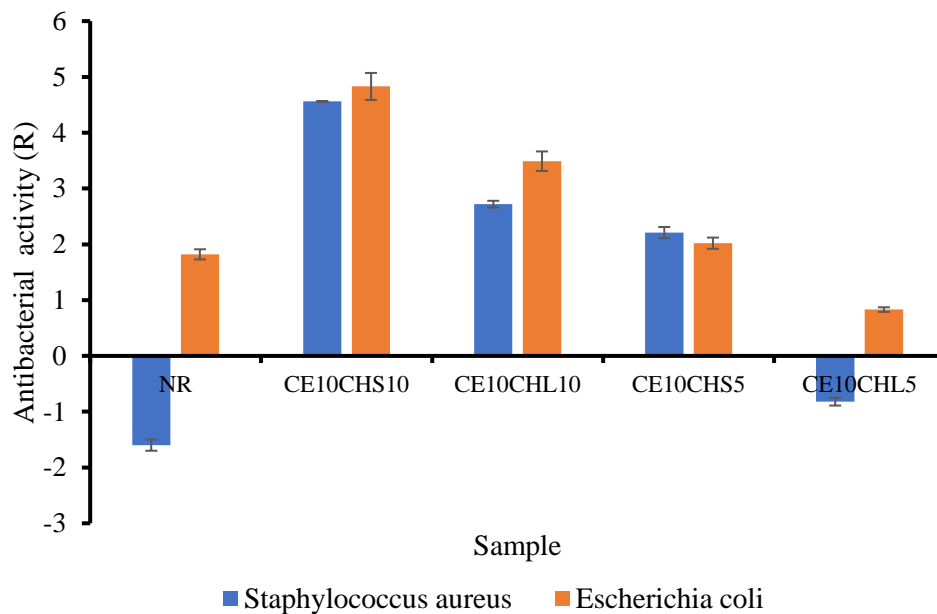


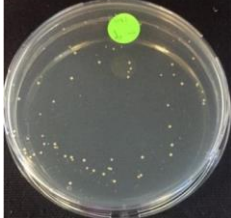
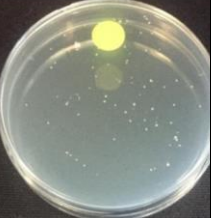

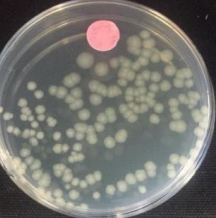
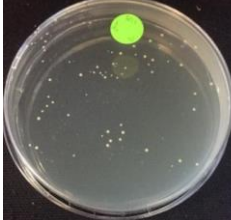
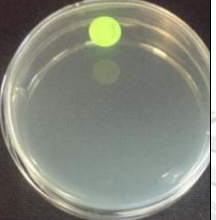

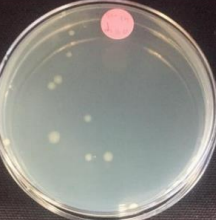
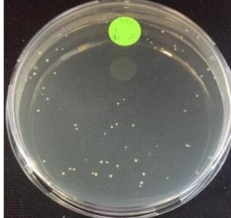
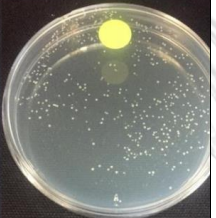


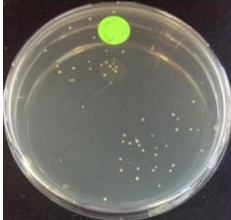
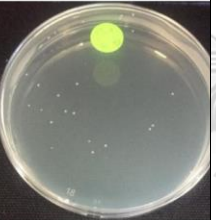
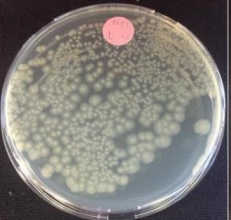
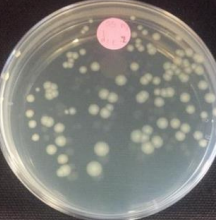
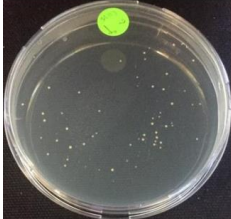
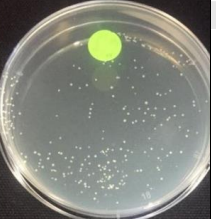


Figure 24 Reduction of *Staphylococcus aureus* and *Escherichia coli* for determining the viable microorganisms validation for the NR and CE/CH/NR composite films.



* Antibacterial activity (R) ≥ 2 exhibit to effective in inhibiting microorganisms.

Figure 25 Antibacterial ability of *Staphylococcus aureus* and *Escherichia coli* for determining the viable microorganisms validation for the NR and CE/CH/NR composite films

Table 10 The clear zone of Staphylococcus aureus and Escherichia coli for determining the viable microorganisms validation for the NR and CE/CH/NR composite films.

Sample	Staphylococcus aureus		Escherichia coli	
	0 h	24 h	0 h	24 h
NR				
CE10CHS10				
CE10CHL10				
CE10CHS5				
CE10CHL5				

CHAPTER V

CONCLUSION

The CE/CH/NR composite films were successfully prepared via latex aqueous microdispersion. Cellulose and chitosan at 5-10%wt could disperse homogeneously within NR matrix. The mechanical properties were effectively enhanced by the reinforcement of cellulose and chitosan. The highest tensile strength and Young's modulus were obtained from the composite film of CE10CHS10, which were approximately 13.8 MPa and 12.74 MPa, respectively. Moreover, CE10CHL5 composite film performed the highest elastic elongation at 526%.

The hydrophilicity of the composite films increased when cellulose and chitosan were added to the NR matrix. The dispersion of cellulose and chitosan in natural rubber matrix and the interfacial interactions of cellulose, chitosan, and NR leads to the improvement in mechanical properties, thermal properties, chemical stability, and antibacterial. The maximum antibacterial activity (R) at 4.56 against *S. aureus* and 4.83 against *E. coli* was obtained from CE10CHS10. A spectacular improvement in mechanical properties and better chemical stability are expected to regard application in green rubber-based products and elastic packaging.

REFERENCES

1. Li H, Yang J, Chen G, Liu X, Zhang Z, et al. 2020. Towards intelligent design optimization: Progress and challenge of design optimization theories and technologies for plastic forming. *Chinese Journal of Aeronautics*
2. Luzi F, Torre L, Kenny J, Puglia D. 2019. Bio- and Fossil-Based Polymeric Blends and Nanocomposites for Packaging: Structure–Property Relationship. *Materials* 12:471
3. Pojanavaraphan T, Magaraphan R. 2008. Pre vulcanized natural rubber latex/clay aerogel nanocomposites. *European Polymer Journal* 44:1968-77
4. Wang J, Chen D. 2013. Mechanical Properties of Natural Rubber Nanocomposites Filled with Thermally Treated Attapulgit. *Journal of Nanomaterials* 2013:496584
5. Sanjay MR, Madhu P, Jawaid M, Sentharamaikkannan P, Senthil S, Pradeep S. 2018. Characterization and properties of natural fiber polymer composites: A comprehensive review. *Journal of Cleaner Production* 172:566-81
6. Klemm D, Heublein B, Fink H-P, Bohn A. 2005. Cellulose: Fascinating Biopolymer and Sustainable Raw Material. *Angewandte Chemie International Edition* 44:3358-93
7. Phomrak S, Phisalaphong M. 2017. Reinforcement of Natural Rubber with Bacterial Cellulose via a Latex Aqueous Microdispersion Process. *Journal of Nanomaterials* 2017:4739793
8. Fouda M, Wittke R, Knittel D, Schollmeyer E. 2009. Use of chitosan/polyamine biopolymers based cotton as a model system to prepare antimicrobial wound dressing. *International Journal of Diabetes Mellitus* 1:61-4
9. Varma AJ, Deshpande SV, Kennedy JF. 2004. Metal complexation by chitosan and its derivatives: a review. *Carbohydrate Polymers* 55:77-93
10. Rinaudo M. 2006. Chitin and chitosan: Properties and applications. *Progress in Polymer Science* 31:603-32
11. Yang J, Kwon G, Hwang K, Kim D-Y. 2018. Cellulose–Chitosan Antibacterial Composite Films Prepared from LiBr Solution. *Polymers* 10:1058
12. H.P.S AK, Saurabh CK, A.S A, Nurul Fazita MR, Syakir MI, et al. 2016. A review on chitosan-cellulose blends and nanocellulose reinforced chitosan biocomposites: Properties and their applications. *Carbohydrate Polymers* 150:216-26
13. Boonrasri S, Sae–Oui P, Rachtanapun P. 2020. Chitosan and Natural Rubber Latex Biocomposite Prepared by Incorporating Negatively Charged Chitosan Dispersion. *Molecules* 25
14. Gutiérrez-Martínez P, Chacón-López A, Xoca-Orozco LA, Ramos-Guerrero A, Velázquez-Estrada R, Aguilera-Aguirre S. 2016. Chapter 11 - Chitosan and Changes in Gene Expression During Fruit–Pathogen Interaction at Postharvest Stage. In *Chitosan in the Preservation of Agricultural Commodities*, ed. S Bautista-Baños, G Romanazzi, A Jiménez-Aparicio:299-311. San Diego: Academic Press. Number of 299-311 pp.
15. Ferreira M, Mendonça RJ, Coutinho-Netto J, Mulato M. 2009. Angiogenic properties of natural rubber latex biomembranes and the serum fraction of *Hevea brasiliensis*. *Brazilian Journal of Physics* 39:564-9

16. Geng C-z, Hu X, Yang G-h, Zhang Q, Chen F, Fu Q. 2015. Mechanically reinforced chitosan/cellulose nanocrystals composites with good transparency and biocompatibility. *Chinese Journal of Polymer Science* 33:61-9
17. Cao L, Fu X, Xu C, Yin S, Chen Y. 2017. High-performance natural rubber nanocomposites with marine biomass (tunicate cellulose). *Cellulose* 24:2849-60
18. Ogawa Y, Azuma K, Izawa H, Morimoto M, Ochi K, et al. 2017. Preparation and biocompatibility of a chitin nanofiber/gelatin composite film. *International Journal of Biological Macromolecules* 104:1882-9
19. Updegraff DM. 1969. Semimicro determination of cellulose in biological materials. *Analytical Biochemistry* 32:420-4
20. Saxena IM, Brown RM. 2001. Biosynthesis of Cellulose. In *Progress in Biotechnology*, ed. N Morohoshi, A Komamine, 18:69-76: Elsevier. Number of 69-76 pp.
21. Abraham E, Deepa B, Pothan LA, John M, Narine SS, et al. 2013. Physicomechanical properties of nanocomposites based on cellulose nanofibre and natural rubber latex. *Cellulose* 20:417-27
22. Sarath CC, Shanks RA, Thomas S. 2014. Chapter 1 - Polymer Blends. In *Nanostructured Polymer Blends*, ed. S Thomas, R Shanks, S Chandrasekharakurup:1-14. Oxford: William Andrew Publishing. Number of 1-14 pp.
23. Tharanathan RN. 2003. Biodegradable films and composite coatings: past, present and future. *Trends in Food Science & Technology* 14:71-8
24. Ma X, Chang PR, Yu J, Stumborg M. 2009. Properties of biodegradable citric acid-modified granular starch/thermoplastic pea starch composites. *Carbohydrate Polymers* 75:1-8
25. Boonmahitthisud A, Boonkerd K. 2021. Sustainable development of natural rubber and its environmentally friendly composites. *Current Opinion in Green and Sustainable Chemistry* 28:100446
26. Rao V, Johns J. 2008. Mechanical properties of thermoplastic elastomeric blends of chitosan and natural rubber latex. *Journal of Applied Polymer Science* 107:2217-23
27. Visakh PM, Thomas S, Oksman K, Mathew AP. 2012. Crosslinked natural rubber nanocomposites reinforced with cellulose whiskers isolated from bamboo waste: Processing and mechanical/thermal properties. *Composites Part A: Applied Science and Manufacturing* 43:735-41
28. Venugopal B, Gopalakrishnan J. 2018. Reinforcement of natural rubber using cellulose nanofibres isolated from Coconut spathe. *Materials Today: Proceedings* 5:16724-31
29. Kumagai A, Tajima N, Iwamoto S, Morimoto T, Nagatani A, et al. 2019. Properties of natural rubber reinforced with cellulose nanofibers based on fiber diameter distribution as estimated by differential centrifugal sedimentation. *International Journal of Biological Macromolecules* 121:989-95
30. Cao L, Yuan D, Fu X, Chen Y. 2018. Green method to reinforce natural rubber with tunicate cellulose nanocrystals via one-pot reaction. *Cellulose* 25:4551-63
31. Blanchard R, Ogunsona EO, Hojabr S, Berry R, Mekonnen TH. 2020. Synergistic Cross-linking and Reinforcing Enhancement of Rubber Latex with Cellulose Nanocrystals for Glove Applications. *ACS Applied Polymer Materials*

- 2:887-98
32. Ding B, Huang S, Shen K, Hou J, Gao H, et al. 2019. Natural rubber bio-nanocomposites reinforced with self-assembled chitin nanofibers from aqueous KOH/urea solution. *Carbohydrate Polymers* 225:115230
 33. Nie J, Mou W, Ding J, Chen Y. 2019. Bio-based epoxidized natural rubber/chitin nanocrystals composites: Self-healing and enhanced mechanical properties. *Composites Part B: Engineering* 172:152-60
 34. Sukthawon C, Dittanet P, Saeoui P, Loykulnant S, Prapainainar P. 2020. Electron beam irradiation crosslinked chitosan/natural rubber -latex film: Preparation and characterization. *Radiation Physics and Chemistry* 177:109159
 35. Xu A, Wang Y, Xu X, Xiao Z, Liu R. 2020. A Clean and Sustainable Cellulose-Based Composite Film Reinforced with Waste Plastic Polyethylene Terephthalate. *Advances in Materials Science and Engineering* 2020:7323521
 36. Jain N, Singh VK, Chauhan S. 2017. A review on mechanical and water absorption properties of polyvinyl alcohol based composites/films. *Journal of the Mechanical Behavior of Materials* 26:213-22
 37. Cazón P, Vázquez M. 2020. Mechanical and barrier properties of chitosan combined with other components as food packaging film. *Environmental Chemistry Letters* 18:257-67
 38. Fan L, Zhang H, Gao M, Zhang M, Liu P, Liu X. 2020. Cellulose nanocrystals/silver nanoparticles: in-situ preparation and application in PVA films. *Holzforchung* 74:523-8
 39. Wardhono EY, Wahyudi H, Agustina S, Oudet F, Pinem MP, et al. 2018. Ultrasonic Irradiation Coupled with Microwave Treatment for Eco-friendly Process of Isolating Bacterial Cellulose Nanocrystals. *Nanomaterials (Basel)* 8:859
 40. Ming-zhe L, Li-feng W, Lei F, Pu-wang L, Si-dong L. 2017. Preparation and properties of natural rubber/chitosan microsphere blends. *Micro & Nano Letters* 12:386-90
 41. Xu C, Wu W, Nie J, Fu L, Lin B. 2019. Preparation of carboxylic styrene butadiene rubber/chitosan composites with dense supramolecular network via solution mixing process. *Composites Part A: Applied Science and Manufacturing* 117:116-24
 42. Czaja W, Romanovicz D, Brown Rm. 2004. Structural investigations of microbial cellulose produced in stationary and agitated culture. *Cellulose* 11:403-11
 43. Weng R, Chen L, Lin S, Zhang H, Wu H, et al. 2017. Preparation and Characterization of Antibacterial Cellulose/Chitosan Nanofiltration Membranes. *Polymers* 9:116
 44. Krlevich ML, Koenig JL. 1998. FTIR Analysis of Silica-Filled Natural Rubber. *Rubber Chemistry and Technology* 71:300-9
 45. Atykyan N, Revin V, Shutova V. 2020. Raman and FT-IR Spectroscopy investigation the cellulose structural differences from bacteria *Gluconacetobacter sucrofermentans* during the different regimes of cultivation on a molasses media. *AMB Express* 10:84
 46. Osman Z, Arof AK. 2003. FTIR studies of chitosan acetate based polymer electrolytes. *Electrochimica Acta* 48:993-9

47. Sivaselvi K, Varma VS, Harikumar A, Jayaprakash A, Sankar S, et al. 2021. Improving the mechanical properties of natural rubber composite with carbon black (N220) as filler. *Materials Today: Proceedings* 42:921-5
48. Thomas MG, Abraham E, Jyotishkumar P, Maria HJ, Pothen LA, Thomas S. 2015. Nanocelluloses from jute fibers and their nanocomposites with natural rubber: Preparation and characterization. *International journal of biological macromolecules* 81:768-77
49. Zhang Z, Jin F, Wu Z, Jin J, Li F, et al. 2017. O-acylation of chitosan nanofibers by short-chain and long-chain fatty acids. *Carbohydrate Polymers* 177:203-9
50. Nam YS, Park WH, Ihm D, Hudson SM. 2010. Effect of the degree of deacetylation on the thermal decomposition of chitin and chitosan nanofibers. *Carbohydrate Polymers* 80:291-5
51. Scott CE, Macosko CW. 1995. Morphology development during the initial stages of polymer-polymer blending. *Polymer* 36:461-70
52. George J, Ramana KV, Sabapathy SN, Jagannath JH, Bawa AS. 2005. Characterization of chemically treated bacterial (*Acetobacter xylinum*) biopolymer: Some thermo-mechanical properties. *International Journal of Biological Macromolecules* 37:189-94
53. Moussout H, Ahlafi H, Aazza M, Bourakhouadar M. 2016. Kinetics and mechanism of the thermal degradation of biopolymers chitin and chitosan using thermogravimetric analysis. *Polymer Degradation and Stability* 130:1-9
54. Ho CC, Khew MC. 2000. Low Glass Transition Temperature (T_g) Rubber Latex Film Formation Studied by Atomic Force Microscopy. *Langmuir* 16:2436-49
55. Bendahou A, Kaddami H, Dufresne A. 2010. Investigation on the effect of cellulosic nanoparticles' morphology on the properties of natural rubber based nanocomposites. *European Polymer Journal* 46:609-20
56. Honary S, Orafai H. 2002. The Effect of Different Plasticizer Molecular Weights and Concentrations on Mechanical and Thermomechanical Properties of Free Films. *Drug Development and Industrial Pharmacy* 28:711-5
57. Wu Y, Lu W-P, Wang J, Gao Y, Guo Y. 2017. Rapid and Convenient Separation of Chitooligosaccharides by Ion-Exchange Chromatography. *IOP Conference Series: Materials Science and Engineering* 275:012008
58. Osorio-Madrado A, David L, Trombotto S, Lucas JM, Peniche-Covas C, Domard A. 2010. Kinetics study of the solid-state acid hydrolysis of chitosan: evolution of the crystallinity and macromolecular structure. *Biomacromolecules* 11:1376-86
59. Gimenez-Dejoz J, Tsunoda K, Fukushima Y, Numata K. 2021. Computational study of the interaction between natural rubber α -terminal groups and l-quebrachitol, one of the major components of natural rubber. *Polymer Journal*
60. Tanrattanakul V, Wattanathai B, Tiangjunya A, Muhamud P. 2003. In situ epoxidized natural rubber: Improved oil resistance of natural rubber. *Journal of Applied Polymer Science* 90:261-9
61. Castro C, Zuluaga R, Álvarez C, Putaux JL, Caro G, et al. 2012. Bacterial cellulose produced by a new acid-resistant strain of *Gluconacetobacter* genus. *Carbohydr Polym* 89:1033-7
62. Lin W-C, Lien C-C, Yeh H-J, Yu C-M, Hsu S-h. 2013. Bacterial cellulose and bacterial cellulose–chitosan membranes for wound dressing applications.

- Carbohydrate Polymers* 94:603-11
63. Ul-Islam M, Khan T, Park JK. 2012. Water holding and release properties of bacterial cellulose obtained by in situ and ex situ modification. *Carbohydrate Polymers* 88:596-603
64. Yu P, He H, Luo Y, Jia D, Dufresne A. 2017. Reinforcement of Natural Rubber: The Use of in Situ Regenerated Cellulose from Alkaline–Urea–Aqueous System. *Macromolecules* 50:7211-21
65. Fortunati E, Luzi F, Puglia D, Terenzi A, Vercellino M, et al. 2013. Ternary PVA nanocomposites containing cellulose nanocrystals from different sources and silver particles: part II. *Carbohydr Polym* 97:837-48
66. Goy R, Britto D, Assis O. 2009. A Review of the Antimicrobial Activity of Chitosan. *Polimeros-ciencia E Tecnologia - POLIMEROS* 19
67. Liu N, Chen XG, Park HJ, Liu CG, Liu CS, et al. 2006. Effect of MW and concentration of chitosan on antibacterial activity of Escherichia coli. *Carbohydrate polymers*. 64:60-5
68. Chawla SP, Kanatt SR, Sharma AK. 2021. Chitosan. In *Polysaccharides: Bioactivity and Biotechnology*, ed. KG Ramawat, J-M Méillon:1-24. Cham: Springer International Publishing. Number of 1-24 pp.





จุฬาลงกรณ์มหาวิทยาลัย
CHULALONGKORN UNIVERSITY

VITA

NAME Naipaporn Sutipanwihan
DATE OF BIRTH 26 July 1997
PLACE OF BIRTH Bangkok
INSTITUTIONS ATTENDED Chulalongkorn University



จุฬาลงกรณ์มหาวิทยาลัย
CHULALONGKORN UNIVERSITY